

Principal components analysis of Laplacian waveforms as a generic method for identifying ERP generator patterns: I. Evaluation with auditory oddball tasks[☆]

Jürgen Kayser^{a,b,*}, Craig E. Tenke^{a,b}

^a Department of Biopsychology, New York State Psychiatric Institute, New York, NY, USA

^b Department of Psychiatry, College of Physicians & Surgeons of Columbia University, New York, NY, USA

Accepted 17 August 2005

Available online 13 December 2005

Abstract

Objective: To evaluate the effectiveness and comparability of PCA-based simplifications of ERP waveforms versus their reference-free Laplacian transformations for separating task- and response-related ERP generator patterns during auditory oddball tasks.

Methods: Nose-referenced ERPs (31 sites total) were recorded from 66 right-handed adults during oddball tasks using syllables or tones. Response mode (left press, right press, silent count) and task was varied within subjects. Spherical spline current source density (CSD) waveforms were computed to sharpen ERP scalp topographies and eliminate volume-conducted contributions. ERP and CSD data were submitted to separate covariance-based, unrestricted temporal PCAs (Varimax) to disentangle temporally and spatially overlapping ERP and CSD components.

Results: Corresponding ERP and CSD factors were unambiguously related to known ERP components. For example, the dipolar organization of a central N1 was evident from factorized anterior sinks and posterior sources encompassing the Sylvian fissure. Factors associated with N2 were characterized by asymmetric frontolateral (tonal: frontotemporal R>L) and parietotemporal (phonetic: parietotemporal L>R) sinks for targets. A single ERP factor summarized parietal P3 activity, along with an anterior negativity. In contrast, two CSD factors peaking at 360 and 560 ms distinguished a parietal P3 source with an anterior sink from a centroparietal P3 source with a sharply localized Fz sink. A smaller parietal but larger left temporal P3 source was found for silent count compared to button press. Left or right press produced opposite, region-specific asymmetries originating from central sites, modulating the N2/P3 complex.

Conclusions: CSD transformation is shown to be a valuable preprocessing step for PCA of ERP data, providing a unique, physiologically meaningful solution to the ubiquitous reference problem. By reducing ERP redundancy and producing sharper, simpler topographies, and without losing or distorting any effects of interest, the CSD-PCA solution replicated and extended previous task- and response-related findings.

Significance: Eliminating ambiguities of the recording reference, the combined CSD-PCA approach systematically bridges between montage-dependent scalp potentials and distinct, anatomically-relevant current generators, and shows promise as a comprehensive, generic strategy for ERP analysis.

© 2005 International Federation of Clinical Neurophysiology. Published by Elsevier Ireland Ltd. All rights reserved.

Keywords: Event-related potential (ERP); Principal components analysis (PCA); Current source density (CSD); Oddball task; Silent counting; Response hand

1. Introduction

Event-related potentials (ERPs) measure time-locked field potentials extracted from the scalp-recorded electroencephalogram (EEG), and, when embedded in a suitable paradigm, allow the combined study of neuronal activity and information processing within a millisecond time

[☆]A preliminary summary of this report has been presented at the 42nd Annual Meeting of the Society for Psychophysiological Research (SPR), October 2002, Washington, DC.

* Corresponding author. Jürgen Kayser, Department of Biopsychology, New York State Psychiatric Institute, Unit 50, 1051 Riverside Drive, New York, NY 10032, USA. Tel.: +1 212 543 5169; fax: +1 212 543 6540.

E-mail address: kayserj@pi.cpmc.columbia.edu (J. Kayser).

resolution (e.g. Picton et al., 2000). Recent improvements in EEG technology, which enable quick application of even dense electrode montages of 128 or more recording channels, have made ERPs a readily-available, inexpensive, and non-invasive tool, rendering it among the most commonly-used psychophysiological measures for the study of human cognition (e.g. Gevins, 1998). Despite its popularity in both basic and clinical research, by comparison, less attention has been paid to two crucial methodological choices affecting the measurement of an ERP component (or any equivalent construct) and the association to its neuronal generation: (1) the procedure for identifying and quantifying relevant ERP components, and (2) the effects of an active EEG recording reference.

1.1. Data-driven ERP component identification and measurement by means of PCA

The construct of an ERP component is used to decompose and understand ERP waveforms by both their intracerebral origin (i.e. underlying neuronal generators) and any experimental manipulations (e.g. Picton et al., 2000), thereby associating characteristic ERP constituents with a specific function (i.e. a perceptual, attentional, or cognitive process) and a specific neuronal activation pattern. This theoretical concept of an ERP component must be distinguished from an observational definition of an ERP component (Donchin et al., 1978), ranging from very simplistic (e.g. peak amplitude, peak latency, area measurements) to more sophisticated approaches (e.g. independent component analysis). One frequently-used, systematic approach of reducing the ERP data dimensionality has been principal components analysis (PCA), which decomposes a set of ERP waveforms into a set of orthogonal constituents (e.g. Chapman and McCrary, 1995; Donchin, 1966; Donchin and Heffley, 1978; Glaser and Ruchkin, 1976; van Boxtel, 1998).

While traditional ERP peak and area measures are subject to experimenter bias (e.g. determining area integration or peak detection limits for deflections that invert and shift across scalp recording locations), PCA can instead be used as an objective, heuristic tool to determine 'data-driven' ERP components measures (e.g. Donchin and Heffley, 1978; Kayser and Tenke, 2003). This procedure identifies and groups unique variance patterns in the raw data, which are not necessarily evident in grand mean ERP averages, or are impossible to comprehend with ERP visualization tools available to a researcher, who is easily overwhelmed by the temporal and spatial complexity of even a modestly-scaled multichannel data set. Thus, PCA serves a two-fold purpose: to identify ERP components of relevance for a given data set, and to generate efficient measurements for these temporally and spatially overlapping components. The resulting components (i.e. factor loadings or factor waveforms) together with their associated weights (i.e. topography of factor scores) can be interpreted as observational definitions of ERP components, if their

characteristics comply with common knowledge of ERP components, vary directly as a function of the experimental manipulation, or can otherwise be meaningfully related to ERP activity that is evident in the averaged waveforms (Kayser and Tenke, 2003). Such an interpretation is possible because of the a priori known organization of the data (i.e. the ERP variables submitted to the PCA are ordered in the temporal and/or spatial domain). Thus, the researcher's subjectivity is reduced to determining the appropriateness of the observed ERP measures, provided in form of PCA component scores, rather than to identifying an ERP measure and justifying its appropriateness.

We have recently shown that unrestricted PCA solutions, when combined with Varimax rotation to achieve simple structure but maintaining factor orthogonality, are particularly helpful in accomplishing this goal (Kayser and Tenke, 2003). Firstly, all restricted solutions converge on an unrestricted PCA solution, independent of the association matrix used for factor extraction (i.e. correlation or covariance matrix). Secondly, unrestricted factor extraction improves the interpretability of high-variance factors and yields stable test statistics typically performed on the factor scores (i.e. *F* values that are not affected but the arbitrary choice for a factor retention criterion). It is a particular advantage of this unrestricted PCA approach that components can gather variance not systematically related to the experimental manipulations (e.g. stemming from physiological and other systematic artifact sources). The separation of artifactual variance contributions from meaningful ERP variance is a very desirable PCA characteristic, as unsystematic variance that is effectively filtered from the data can no longer obscure effects of primary interest.

The use of PCA for the analysis of ERP data has been disputed because of the risk of a misallocation of variance saliently demonstrated in a simulation study by Wood and McCarthy (1984), although these authors themselves noted that traditional measures are subject to the very same pitfall. In fact, when using a more realistic test power and also simulating a realistic component topography, misallocation of variance is greatly reduced for PCA-derived component measures, and baseline-to-peak measures are equally or even more prone to this problem (Beauducel and Debener, 2003). When directly compared within the same data set, PCA-based component measures yielded larger effect sizes than time window integrals (Kayser et al., 1998) and better reliabilities than peak-based amplitudes (Beauducel et al., 2000). The use of PCA is not a protection against poor ERP data quality stemming from low signal-to-noise ratios, outliers, or temporal or spatial jitter (e.g. Chapman and McCrary, 1995; Dien, 1998a; Donchin and Heffley, 1978; van Boxtel, 1998), although it may alert the researcher to serious data problems, which sometimes may even be counteracted by exploiting the linear properties of PCA (e.g. reducing blink artifacts; Casarotto et al., 2004). Therefore, like traditional ERP measures, PCA solutions are dependent

on the characteristics of the raw data, the choice of the recording reference being prominent among many possible methodological variations.

1.2. *The impact of the recording reference for volume-conducted surface potentials*

The recording of electrical activity from scalp involves the measurement of a potential difference between at least two sites, with one serving as the reference and, therefore, being arbitrarily set to zero. However, no recording site placed anywhere on the human body can be considered neutral or electrically inactive, including cephalic (e.g. mastoid, nose, ear lobe, vertex, average, etc.) and non-cephalic (sternum, neck, etc.) sites or combination thereof, and any site will be (differentially) affected by a given combination of neuronal generators through volume-conducted activity (e.g. Nunez, 1981; Nunez and Westdorp, 1994). Although equally true for all ERP components, a typical example are the generators of the auditory N1 located in dorsal-superior portions of the temporal lobe (Heschl's gyrus, AII, superior temporal gyrus, planum temporale; e.g. Liegeois-Chauvel et al., 1994; Näätänen and Picton, 1987; Pantev et al., 1995; Simson et al., 1976), which will produce different polarities, amplitudes, and even peak latencies at all recording sites when the recording reference is systematically varied within the EEG montage. The choice of the recording reference is, therefore, essential for identifying both spatial and temporal information of ERP recordings, as the reference like any other recording site will invariably reflect the spatio-temporal activation of ERP generator patterns to a certain degree. Whereas some reference choices may enhance or reduce any particular generator topography, all physically-realizable recording reference schemes, including a montage-dependent average reference, are subject to the very same reference problem (e.g. Desmedt and Tomberg, 1990; Dien, 1998b; Junghöfer et al., 1999; Pascual-Marqui and Lehmann, 1993; Tomberg et al., 1990). By acknowledging the interpretational problems stemming from an arbitrary choice of a recording reference, and to facilitate the comparison of findings across studies using a different reference scheme, ERP waveforms are sometimes rereferenced to two or more common reference schemes (e.g. Kayser et al., 1997; 2003a). The use of multiple reference schemes may help to improve the appreciation of distinct ERP components, which can be differentially affected by different references.

Recently, a reference electrode standardization technique estimating a reference potential at infinity from the recorded EEG has been proposed to solve this problem (Yao, 2001; Zhai and Yao, 2004). While this new reference-free approach, which is based on an equivalent distributed source model, may be appealing and promising, several

volume-conduction algorithms have previously been proposed to yield reference-free data transformations (e.g. Hjorth, 1975; 1980; Perrin et al., 1989; Yao, 2002a), thereby circumventing problems associated with the choice of a recording reference. Also known as current source density (CSD) transformations, these algorithms compute an estimate of the current injected radially into the skull and scalp from the underlying neuronal tissue (i.e. the scalp Laplacian) at a given surface location, from a spatially weighted sum of the potential gradients directed at this site from all recording sites (see Tenke and Kayser, 2005, for a detailed discussion). The central transformation common to all CSD algorithms is derived from the negative second spatial derivative of the interpolated scalp surface potentials, which approximates the true scalp Laplacian for low spatial frequencies (Yao, 2002b). CSD maps represent the magnitude of the radial (transcranial) current flow entering (sources) and leaving (sinks) the scalp (Nunez, 1981). The benefits of a CSD transform are a reference-free, spatially-enhanced representation of the direction, location, and intensity of current generators that underlie an ERP topography (Nicholson, 1973; Mitzdorf, 1985). CSD methods have been shown to provide an empirically useful means of simplifying the topographies of ERP components (e.g. Law et al., 1993). By virtue of the algorithm, any surface potential reference montage will produce identical CSD waveforms.

In the context of cognitive ERP research, CSD methods have largely been used to better understand the topography of radial currents that underlie the recorded surface potentials, often only as an additional visualization tool for predetermined ERP components measures (e.g. base-to-peak amplitudes or integrated time windows), thereby focusing on the spatial benefits (i.e. sharper representation, interpolation of undersampled scalp regions). For instance, we have previously applied a local Hjorth transformation to ERP measures based on principal components analysis (PCA) to identify the most representative sites within a given topography (Kayser et al., 2000a). In contrast, intracranial CSD applications have concentrated on the temporal variation of the neuronal origin of the scalp-recorded field potentials to separate the generator contributions of cortical sublaminae (Buzsaki et al., 1986; Holsheimer, 1987; Nicholson and Freeman, 1975; Mitzdorf, 1985; Schroeder et al., 1992), thereby focusing on CSD waveforms rather than CSD topographies. As the CSD algorithm is discrete in the sense that it can be independently applied to any sample point, the resulting temporal (real-time) sequence of sharpened, reference-free current flow topographies could also be used in cognitive ERP research. Although Tenke et al. (1998) used CSD waveforms to study response-related source asymmetries in an auditory oddball task, these topographic analyses were limited to time window integrals.

1.3. The present study: button press versus silent count in tonal and phonetic oddball tasks

The present report sought to systematically and more comprehensively evaluate the possibility of combining the methodological advantages of reference-free, topographically-enhanced CSD waveforms with the virtues of unrestricted temporal PCA to identify and measure neuronal generators underlying known ERP components. For this purpose, we revisited the issue of dissociated ERP topographies for tonal and phonetic oddball tasks, and their modulation by different response requirements typical for target detection tasks.

Using a conventional 30-channel (Kayser et al., 1998; 2001) or a 128-channel (Kayser et al., 2000b) EEG montage, we have repeatedly found that healthy adults show enhanced N2 and P3 amplitudes over the right lateral-temporal region for complex tones, but enhanced N2 and P3 amplitudes over the left parietal region for consonant-vowel syllables, in auditory target detection (oddball) tasks using these stimuli. As these tonal or phonetic stimuli are also known to produce opposite perceptual performance asymmetries in dichotic listening studies (e.g. Berlin et al., 1973; Bruder, 1995; Sidtis, 1981), we interpreted the stimulus-dependent N2/P3 asymmetries as electrophysiological evidence of differentially activated neuronal networks predominantly involved in pitch discrimination (right fronto-temporal) or phoneme discrimination (left parieto-temporal). Findings and interpretation are consistent with evidence that N2 and P3 jointly reflect endogenous ERP activity associated with the phonemic categorization of speech stimuli (e.g. Maiste et al., 1995), and that the required cognitive task operations depend on a network of regionalized, functionally-specific subprocessors (cf. Gevins et al., 1995). This tonal/phonetic oddball paradigm has been successfully used to probe lateralized neurophysiologic processes underlying cognitive dysfunctions in psychiatric disorders, such as schizophrenia (Kayser et al., 2001) or depression and anxiety (Bruder et al., 2002).

In our previous study (Kayser et al., 1998), we reported that these task-dependent and region-specific ERP asymmetries are also modulated by response requirements (i.e. a button press to target stimuli with either the left or right hand), and that these effects are not merely due to equal asymmetrical, motor-related negativities contralateral to the response hand (e.g. Kutas and Donchin, 1980). A response-related negativity, superimposing cognitive ERP components (i.e. N2 and P3), was evident in target ERPs particularly over frontocentral brain regions. It thereby had a stronger effect on the regional topographies characterizing the tonal task than on the posterior, parietal asymmetries seen for the phonetic task. For instance, N2 amplitude was greater over left than right hemisphere sites in the phonetic task regardless of response hand, whereas the hemispheric asymmetry of N2 for the tonal task was dependent on response hand (Kayser et al., 1998). Furthermore, responding

with the left hand resulted in a greater response-related contralateral negativity than responding with the right hand for right-handed healthy adults (Kayser et al., 1998; Tenke et al., 1998). At the same time, right button presses resulted in greater right-larger-than-left parietal P3 sources compared to left button presses resulting in the opposite asymmetry (Tenke et al., 1998). It would, therefore, be difficult to evaluate task-related topographic effects in the context of a classic oddball paradigm if all responses are made by one hand because motor- or response-related potentials may contaminate the findings. However, it should be carefully noted that in these studies response hand was manipulated between- rather than within-subjects, and that response-related findings may be subject to random selection effects given the relatively small sample size typical for ERP studies.

Frequently, a silent (mental) count instead of a manual response is required in target detection tasks, which avoids motor-related confounds altogether. Several studies have reported an impact of response mode requirements on prominent cognitive ERP components during target detection (e.g. Lew and Polich, 1993; Polich, 1987; Starr et al., 1997), but it is not completely clear whether these differences should be interpreted in terms of attentional resources, movement control, or both. In fact, Salisbury et al. (2001, 2004) have argued that button pressing relative to silent counting distorts the typical P3 topography (although only right button presses were studied), and that ‘increase’ in frontal P3 positivity in NoGo as opposed to Go target responses should be interpreted as a motor-related negativity rather than as a NoGo P3 enhancement reflecting active response inhibition (e.g. Fallgatter and Strik, 1999; Fallgatter et al., 2000; Roberts et al., 1994). While these findings may promote the use of a paradigm that avoids a manual response mode, it is important to recognize two main pitfalls of a silent count condition: (1) a grossly reduced insight into participants’ performance (response latency and item-related accuracy) preventing the exclusion of error trials when computing ERP waveforms, both of which is particularly concerning when groups or conditions under study differ widely in performance level; and (2) the required verbal memory load of the ongoing target count, adding a lateralized, dual-task component to the oddball paradigm (e.g. Friedman and Polson, 1981).

As previous studies have used between-subjects and/or incomplete response mode comparisons (e.g. Kayser et al., 1998; 2001; Salisbury et al., 2001; 2004), this study directly compared the impact of these distinct response mode requirements (silent count, right press, left press) on the topography of ERP components previously observed in tonal and phonetic target detection tasks. The predominant objective was to explore the usefulness of combining CSD and PCA methodology for disentangling known task- and response-related effects by revealing the temporal-spatial dynamic of their underlying generator patterns.

2. Methods

2.1. Participants

EEG data recorded from 66 right-handed, healthy adults (25 men) were selected for this report. These individuals had volunteered to participate in one of two ongoing research studies at the Psychophysiology Laboratory at New York State Psychiatric Institute, which had been approved by the institutional review board, for a monetary compensation of \$15/hr. The experimental protocol, which was undertaken with the understanding and written consent of each participant, was identical in these two studies for the reported tasks. All participants were screened to exclude those with current or past neurologic or psychiatric disorders. Hearing acuity was assessed using standard audiometric procedures, which required all participants to have a difference of less than 10 dB between ears at threshold and a hearing loss no greater than 25 dB at 500, 1,000, or 2,000 Hz. Participants' age ranged from 20 to 51 years (median = 25; mean = 27.3, SD = 6.6), and the mean education level of the sample was 15.5 years (SD = 1.7). The laterality quotient of the Edinburgh Handedness Inventory (Oldfield, 1971), which can vary between -100.0 (completely left-handed) and +100.0 (completely right-handed), was +77.1 (SD = 20.9; range +5.3 to +100.0).

2.2. Stimuli and procedure

The present design was directly derived from our previous studies (Kayser et al., 1998; 2001). Two auditory

target detection (oddball) tasks, using either tonal or phonetic stimuli known to produce opposite perceptual performance asymmetries in dichotic listening studies (e.g. Berlin et al., 1973; Sidtis, 1981), were chosen to probe cognitive processes predominantly performed by the right or left hemisphere. For the tonal task, stimuli consisted of two square waves with fundamental frequencies of 444 and 485 Hz, approximately corresponding to the major notes A4 and B4. These complex tones had a duration of 250 ms with 25 ms rise and decay time (Fig. 1A). For the phonetic task, stimuli consisted of two consonant-vowel syllables (/da/, /ta/) spoken by a male voice. Despite having a more complex frequency composition, syllables were approximately matched to the complex tones by discriminability, duration, and root mean squared amplitude (Fig. 1B). All stimuli were presented binaurally at 72 dB SPL via a matched pair of TDH-49 earphones using STIM software (NeuroScan Inc., 1994). Earphone orientation was counter-balanced across participants.

During twelve experimental 80-trial blocks (960 trials total), participants listened to a series of either tones or syllables with 20% target (16 per block) and 80% nontarget (64 per block) stimuli. All stimuli were presented with a fixed interstimulus interval of 1,750 ms (stimulus onset asynchrony 2,000 ms). Tones or syllables were used as stimuli in half of the blocks, systematically alternating the assignment of target and frequent stimulus in two consecutive blocks (A4 vs. B4, /da/ vs. /ta/). Participants were instructed to respond to infrequent target stimuli as quickly and accurately as possible using one of three response modes: (1) to press the left-most button of a response pad with the left hand; (2) to press

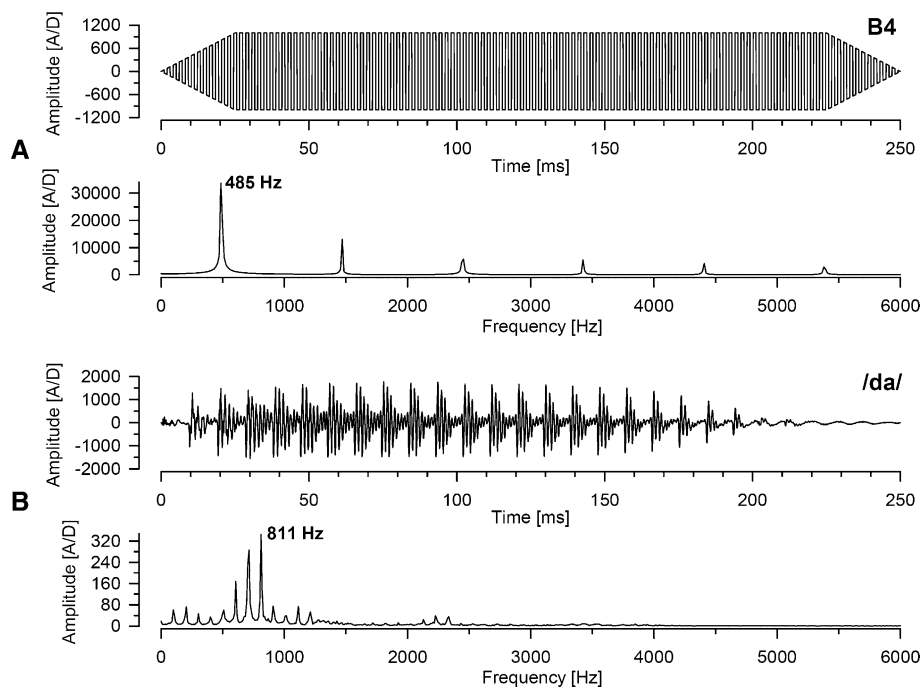


Fig. 1. Examples of (A) tonal and (B) phonetic stimuli, showing time courses and frequency spectra of the complex tone corresponding to the musical note B4 (fundamental frequency 485 Hz) and the consonant-vowel syllable /da/ (peak frequency 811 Hz).

the right-most button of a response pad with the right hand; or (3) to silently count the targets. For the silent count condition, either 15 (65) or 17 (63) targets (nontargets) were used in the stimulus series, and participants reported their target count at the end of the block. The order of these twelve blocks, consisting of two blocks for each combination of response mode (left press [L], right press [R], silent count [S]) with task type (tonal [T], phonetic [P]), was counter-balanced across participants by systematically alternating the orders of task nested under response mode order for any two consecutive blocks (e.g. PL-TL-PR-TR-PS-TS or TL-PL-TS-PS-TR-PR). To reduce ocular artifacts, participants were instructed to fixate a cross on a monitor while listening to the stimuli.

2.3. Data acquisition and recording procedures

Using a Lycra stretch cap (ElectroCap International, Inc.), scalp EEG was recorded from 4 midline (Fz, Cz, Pz, Oz) and 13 lateral pairs of tin electrodes (FP1/2, F3/4, F7/8, FC5/6, FT9/10, C3/4, T7/8, CP5/6, TP9/10, P3/4, P7/8, P9/10, O1/2) with a nose tip reference and an Fpz ground. Standard tin drop electrodes at supra- and infra-orbital sites surrounding the right eye were used to monitor eye blinks and vertical eye movement (bipolar), and electrodes at right and left outer canthi monitored horizontal eye movements (bipolar). All electrode impedances were maintained at or below 5 k Ω . Data were recorded through a Grass Neurodata acquisition system at a gain of 10 k (5 and 2 k for horizontal and vertical eye channels, respectively) with a bandpass of .1–30 Hz (–6 dB/octave). A PC-based EEG acquisition system (Neuroscan) was used to continuously record the data at 200 samples/s during the task. Stimulus trigger codes, responses and response latencies were recorded online along with the EEG data for later analyses. Recording epochs of 1,280 ms (including a 200 ms prestimulus baseline) were extracted off-line, tagged for A/D saturation, and low pass filtered at 20 Hz (–24 dB/octave). Blink activity was effectively corrected using a linear regression algorithm (Semlitsch et al., 1986). Epochs contaminated by amplifier block or drift, residual blinks, lateral eye movements, muscle activity or movement-related artifacts were excluded from analysis by means of a rejection criterion of $\pm 100 \mu\text{V}$ on any channel followed by direct visual inspection of the raw data.

For each participant, average ERP waveforms were separately computed from artifact-free trials (correct responses only for button press) for each of the twelve experimental conditions stemming from the combination of task (tonal, phonetic), response mode (left press, right press, silent count), and oddball stimulus (target, frequent). The mean number of trials used to compute these ERP averages ranged across task and response mode from 26.2 (SD=5.3) to 26.9 (SD=4.8) for targets, and from 104.4 (SD=18.7) to 106.9 (SD=17.4) for nontargets. Visual inspections of

the individual ERP waveforms warranted that the signal-to-noise ratio was satisfactory for each participant and each condition. ERP waveforms were screened for electrolyte bridges (Tenke and Kayser, 2001), digitally low-pass filtered at 12.5 Hz (–24 dB/octave), and finally baseline-corrected using the 100 ms preceding stimulus onset.

2.4. Current source density

All averaged ERP waveforms were transformed into current source density estimates using the spherical spline surface Laplacian algorithm suggested by Perrin et al. (1989, 1990):

$$C(E) = \sum_{i=1}^N c_i h(\cos(E, E_i)) \quad (1)$$

where $C(E)$ is the current density value at any surface point E on a sphere, c_i a computable constant for electrode i of a given montage of N electrodes to account for the set of surface potentials in a spherical model (Perrin et al., 1989), and $\cos(E, E_i)$ denotes the cosine of the angle between a surface point of E and the electrode projection E_i . The function $h(x)$ is defined as the sum of the series (Perrin et al., 1990):

$$h(x) = \frac{1}{4\pi} \sum_{n=1}^{\infty} \frac{2n+1}{n^{m-1}(n+1)^{m-1}} P_n(x) \quad (2)$$

where m is a constant greater than 1, and P_n is the n th Legendre polynomial as defined by (Perrin et al., 1990):

$$\Delta P_n = -n(n+1)P_n \quad (3)$$

A smoothing constant λ is frequently added to the diagonal elements of the cosine matrix $\cos(E_i, E_j)$ of electrode projections E_i and E_j used for the spherical spline interpolation. CSD waveforms were computed for each original surface potential ERP waveform using parameters (50 iterations; $m=4$; $\lambda=10^{-5}$) which have previously been found to yield CSD waveforms similar to local Hjorth Laplacian transformations for all electrodes off the periphery of our 30-channel recording montage (Tenke et al., 1998). A CSD MatLab source code, along with the source code for calculating the spatial electrode locations, is given in the Appendix (Supplementary data, doi:10.1016/j.clinph.2005.08.034) to explicitly state the simple spherical model used for this particular CSD transformation, and also to provide an easy means for ERP researchers to apply these methods to any EEG montage based on the ten-twenty electrode system (Jasper, 1958) and its extensions (Oostenvelde and Praamstra, 2001). Current source density estimates were expressed as the negative surface Laplacian of the ERP at each electrode based on a unit sphere (radius $r=1.0$), and ultimately scaled to Laplacian units ($\mu\text{V}/\text{cm}^2$) based on a more realistic head radius of 10 cm.

2.5. Data reduction and analysis

To determine common sources of variance in the ERP data, the averaged waveforms were submitted to temporal principal components analysis (PCA) derived from the covariance matrix, followed by unscaled Varimax rotation (Kayser and Tenke, 2003). This approach produces distinctive PCA components (i.e. the factor loadings) and corresponding weighting coefficients (i.e. the factor scores), which describe the variance contributions of temporally and spatially overlapping ERP components more efficiently than conventional ERP measures (e.g. yielding larger effect sizes [Kayser et al., 1997, 1998, 1999, 2000a] or higher reliabilities [Beauducel et al., 2000]). The factor scores can be interpreted as weighted time window amplitudes if the associated factor loadings are clustered in a narrow time range and lack significant secondary loadings at different latencies (Kayser et al., 2000a; 2001; Kayser and Tenke, 2003). The correspondence between the time course and topography of PCA factors and ERP components (e.g. N1, N2, P3) allows identification of physiologically-relevant factors for further analysis, which is analogous to the identification of relevant deflections or time intervals from visually inspecting grand mean ERPs (i.e. this approach also uses common ERP knowledge and reasoning), but the latter lacks the ‘data-driven’ objectivity and orthogonality of variance contributions (Kayser and Tenke, 2003; Picton et al., 2000). Although several limitations of PCA techniques (e.g. misallocation of variance resulting from latency jitter or component overlap) are well-known and demand cautious attention, it is important to recognize that peak- or time window-based ERP measures are subject to the very same limitations, but, unlike PCA, these constraints are rarely made explicit (e.g. Achim and Marcantoni, 1997; Beauducel and Debener, 2003; Chapman and McCrary, 1995; Dien, 1998a; Möcks and Verleger, 1986; Wood and McCarthy, 1984).

As a new approach, the same analytic technique was applied to the CSD waveforms, that is, to reference-free transformations of the original ERP waveforms. By analogy, this should result in the extraction of CSD factors closely corresponding to CSD components evident in the CSD waveforms, thereby providing a concise simplification of their temporal and spatial distribution. Unlike ERP factors, these CSD factors are no longer subject to the choice of the recording reference.

Using a MatLab function (appendix of Kayser and Tenke, 2003) that emulates the PCA algorithms used by BMDP statistical software (program 4M; Dixon, 1992), a temporal PCA was computed for each of the two parallel data sets (ERP, CSD) using 220 sample points (–100 to 995 ms) as variables (columns), and 24,552 observations (rows) resulting from the combination of participants (66), stimulus type or task (2), response mode (3), oddball condition (2), and electrode sites (31, including the nose). The number of orthogonal factors extracted and retained for

Varimax rotation was not restricted by any arbitrary criterion, such as the scree test (Cattell, 1966) or various estimates of noise variance (Kaiser, 1960; Horn, 1965). Rather, by allowing the PCA to also extract unsystematic or noise-related components, we have found that the stability of meaningful components is maximized and the risk of false positives in significance tests of the associated factor scores is minimized (Kayser and Tenke, 2003).

2.6. Statistical analysis

As this study introduces a new strategy to process and analyze ERP data, we decided to conduct all statistical analyses in a parallel fashion for the established PCA-ANOVA approach using ERP waveforms (e.g. Chapman and McCrary, 1995) and the novel PCA-ANOVA approach using CSD waveforms. Such a direct comparison should help to better assess the potential benefits or pitfalls of a new analytic strategy, as opposed to an across-study evaluation implicitly founding the verdict on different data sets (e.g. Kayser, Tenke, and Bruder, 2003b).

For each PCA, factor scores for target stimuli were submitted to repeated measures analysis of variance (ANOVA) with task (tonal, phonetic) and response mode (left press, right press, silent count) as a within-subjects factors. Guided by our previous findings (Kayser et al., 1998; 2001), and to increase statistical power for testing a priori hypotheses, repeated measures ANOVA were conducted for subsets of recording sites at which PCA factor scores were largest and most representative of the associated ERP and CSD components. These subsets consisted of either midline or lateral, homologous recording sites over both hemispheres, thus adding either site, or site and hemisphere as within-subjects factors to the design. The rationale for selecting a ‘subset’ of recording sites as a ‘representative’ measure for a factor is given below with the factor descriptions. For this reason, and to avoid needless complexity, site effects are not reported.

Greenhouse-Geisser epsilon (ϵ) correction was used to compensate for violations of sphericity when appropriate (e.g. Keselman, 1998; Picton et al., 2000). The sources of interactions and main effects were systematically examined through contrasts or simple effects (BMDP-4V; Dixon, 1992). A conventional significance level ($P < .05$) was applied for effects involving the two-level design factors task and hemisphere. A more conservative approach was taken with respect to the design factor response mode, which was realized in this study as a three-level, within-subjects factor, rather than as a two-level, between-subjects factor, with silent count adding another response condition not included in our previous studies (Kayser et al., 1998; 2001). To better protect the study against Type 1 errors given the rather large sample ($N=66$), only very robust effects involving response mode ($P < .01$) are reported.

For the behavioral data, button press responses and silently counting were separately analyzed. For button press, response

latency (mean response time of correct responses) and percentages of correct responses were submitted to repeated measures ANOVA with task (tonal, phonetic) and response hand (left, right) as within-subjects factors. For silent count, percentages of correct responses were estimated for each task from the deviation of the reported count from the true number of targets in any trial block (i.e. Hit rate = $(1 - \text{abs}(\text{count} - \text{targets}))/\text{targets}) * 100$).

Gender (male, female) was entered as a control factor in all statistical analyses but will not be considered further in this report.

3. Results

3.1. Behavioral data

Mean response latency for correct button press responses was 20 ms faster for tones ($M=476.6$ ms, $SD=127.8$) compared with syllables ($M=496.0$ ms, $SD=126.0$; task main effect, $F_{[1,64]}=6.18$, $P=.02$), which is in accordance with our previous findings for healthy adults (Kayser et al., 1998; 2001). Conversely, the mean hit rate was approximately 2% lower for tonal ($M=96.9\%$, $SD=7.2$) compared with phonetic stimuli ($M=98.7\%$, $SD=2.6$; task main effect, $F_{[1,64]}=4.65$, $P=.03$); however, this accuracy measure was likely subject to ceiling effects. A highly comparable mean hit rate was observed for silent count,

with no significant differences between tonal ($M=95.4\%$, $SD=8.1$) and phonetic stimuli ($M=96.5\%$, $SD=5.0$; task main effect, $F_{[1,64]}=1.25$, n.s.). No other significant effects evolved from these analyses. As these findings indicate a high accuracy in all response conditions, it was naturally assumed that participants performed on a similarly high level when silently counting targets which precluded direct estimates of response speed and accuracy.

3.2. Average ERP and CSD waveforms

Grand average ERP waveforms of the surface potentials are shown in Fig. 2 separately for the tonal and phonetic task, comparing target stimuli of the three response modes (left press, right press, silent count) with a pooled average of all nontargets. In close correspondence to our previous findings using a nose reference (Kayser et al., 1998; 2001), distinctive ERP components were identified as N1 (peak latency 105 and 115 ms for tonal and phonetic tasks, respectively), P2 for nontargets (between 175 and 195 ms) and N2 for targets (between 200 and 235 ms), P3 (between 355 and 375 ms), a relative negative peak for targets previously labeled N3 (between 490 and 560 ms), and slow wave (beyond 630 ms). The expected condition effects are evident across tasks, revealing N2 and P3 amplitudes for target stimuli only. Across tasks, N1 was most prominent at frontocentral sites (e.g. Cz), although smaller for syllables

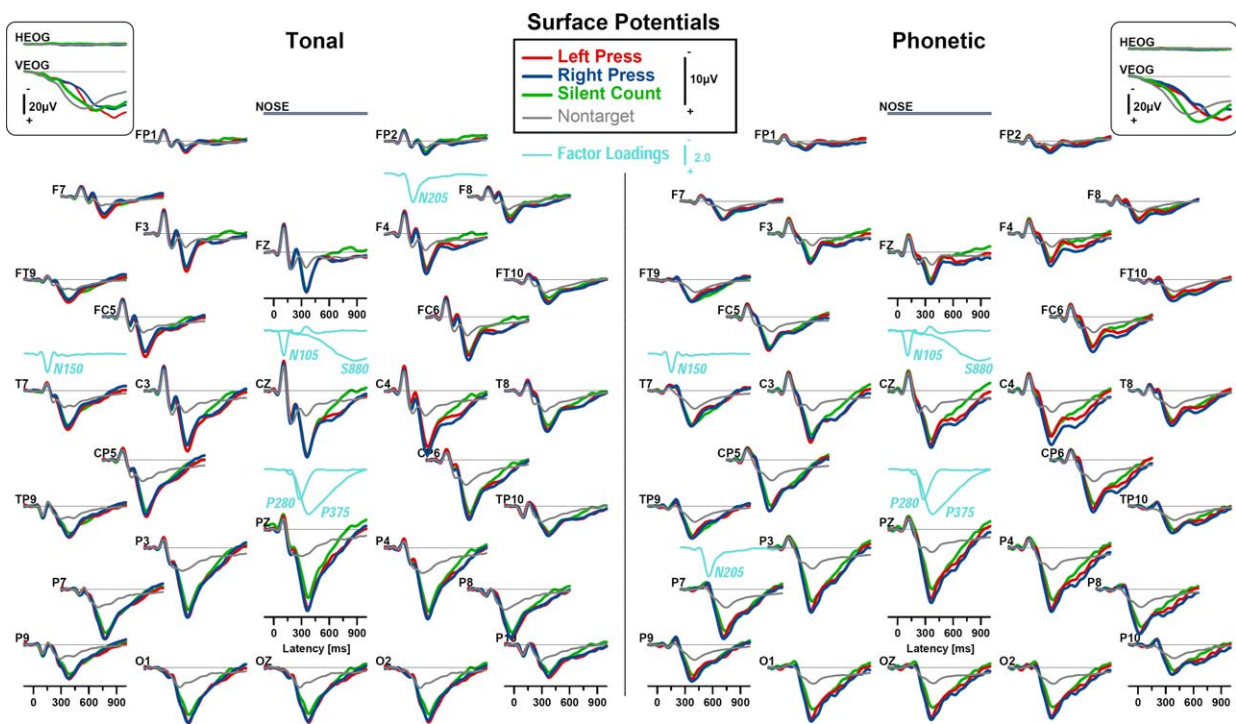


Fig. 2. Grand average event-related potential (ERP) waveforms for 66 healthy adults at all 30 recording sites (using a nose tip reference) for tonal (left) and phonetic (right) stimuli, comparing left press, right press, and silent count targets with nontargets (averaged across response mode). Horizontal (HEOG) and vertical (VEOG) electrooculograms are shown at a smaller scale before blink correction in insets. ERP components were well-defined, including N1, N2, and P3, and closely corresponded to the extracted PCA factors, as is evident from the time course of the ERP factor loadings shown near selected sites. (This figure appears in colour on the web).

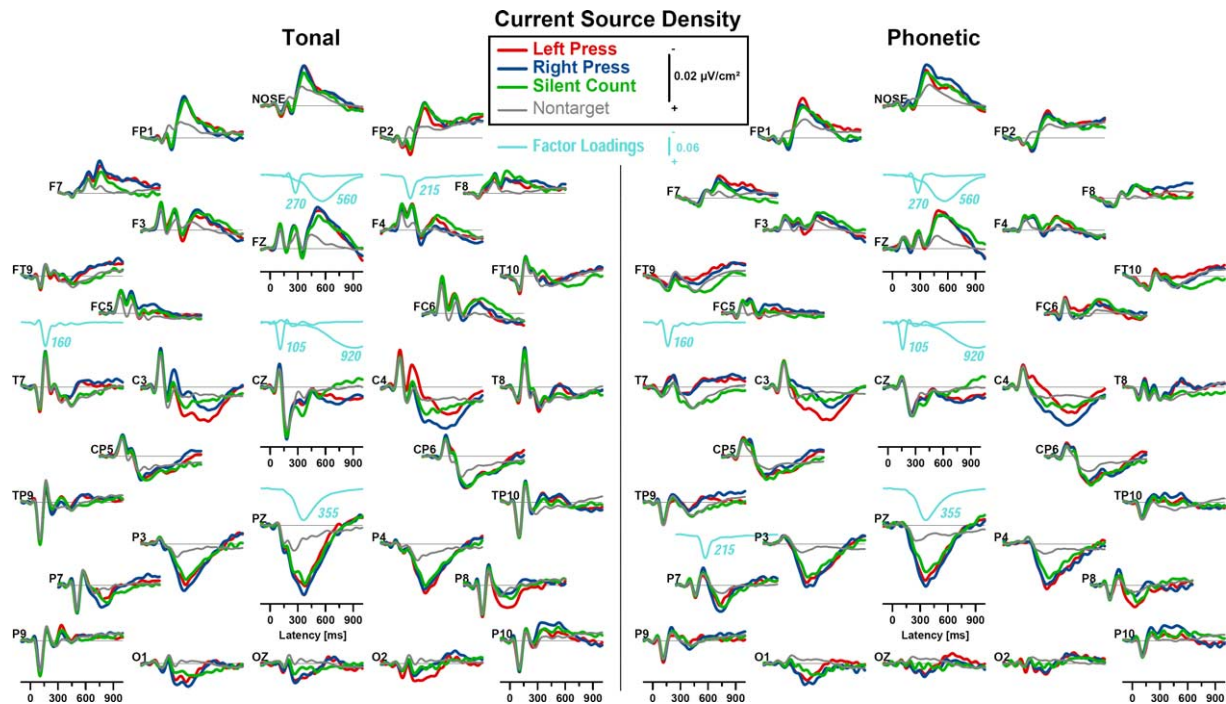


Fig. 3. Reference-free current source density (CSD) waveforms (spherical spline Laplacians; Perrin et al., 1989; 1990) for 66 healthy adults at all 31 recording sites for tonal (left) and phonetic (right) stimuli, comparing left press, right press, and silent count targets with nontargets (averaged across response mode). Distinct CSD components included early mid-central and lateral-temporal sinks, a late mid-parietal source, and a late mid-frontal sink, and closely corresponded to the extracted PCA factors, as is evident from the time course of the CSD factor loadings shown near selected sites. (This figure appears in colour on the web).

compared to tones. N2 was most prominent at lateral sites, encompassing frontal, temporal, and parietal regions (F7/8, FT9/10, T7/8, TP9/10, P7/8, P9/10), being more distinct at frontotemporal sites for tones, and at temporoparietal sites for syllables. P3 was broadly distributed over posterior sites with a maximum over the mid-parietal region (Pz), which was greater in the tonal task.

The reference-free CSD transformations of these ERP waveforms are given in Fig. 3. In order of their peak latencies, distinctive CSD components were: a lateral temporoparietal source corresponding to a central sink (approximate peak latency 100 ms; e.g. see sites TP9/10 and Cz); a lateral temporal sink for tones (155 ms; T7/8) but not for syllables; an early midfrontal sink (between 220 and 290 ms), which was more prominent for targets (e.g. F3/4); a mid-parietal source for targets, corresponding to an anterior sink (between 345 and 380 ms; Pz, Nose); and a late mid-frontal sink for targets (between 480 and 580 ms; Fz). Most notably, CSD waveforms revealed marked button press effects over medial-central sites (C3/4), shifting the contralateral CSD waveforms in negative direction for most of the recording epoch. By comparison, silent count responses showed a relative smaller source activity associated with targets at mid-parietal sites (e.g. Pz).¹

¹ Animated topographies of the grand mean ERP and CSD waveforms shown in Figs. 2 and 3 can be obtained at URL <http://psychophysiology.pmc.columbia.edu/cn2003csd.html>.

3.3. Component waveforms of PCA solutions

A total of 42 and 44 factors were sufficient to completely explain the variance in the ERP and CSD data sets, respectively. Factors were selected for further analysis if they could unambiguously be related to ERP or CSD components through their temporal characteristics (i.e. the peak latencies of the factor loadings) and their spatial configurations (i.e. the factor score topographies for each experimental manipulation; cf. Kayser and Tenke, 2003). ERP factors were labeled to reflect both the peak latency of the factor loadings and the polarity of the associated ERP component; in contrast, CSD factors were labeled using only the peak latency of the factor loadings to avoid confusion. Fig. 4 compares the time courses of the factor loadings for six ERP factors (i.e. factors 1 to 4, 6 and 8 extracted from the surface potentials) with those of the first seven CSD factors. To better relate these PCA component waveforms to the ERP or CSD waveforms, the factor loadings have also been included in Figs. 2 and 3 near selected sites. Five of the six ERP factors, which together accounted for 86.4% of the overall ERP variance after Varimax rotation, closely matched those previously reported for two independent samples of healthy adults for these tonal and phonetic oddball tasks (Kayser et al., 1998; 2001). The first seven CSD factors accounted for 88.6% of the overall CSD variance after Varimax rotation.

It is immediately apparent from Fig. 4 that both PCA solutions produced corresponding factors, with the notable

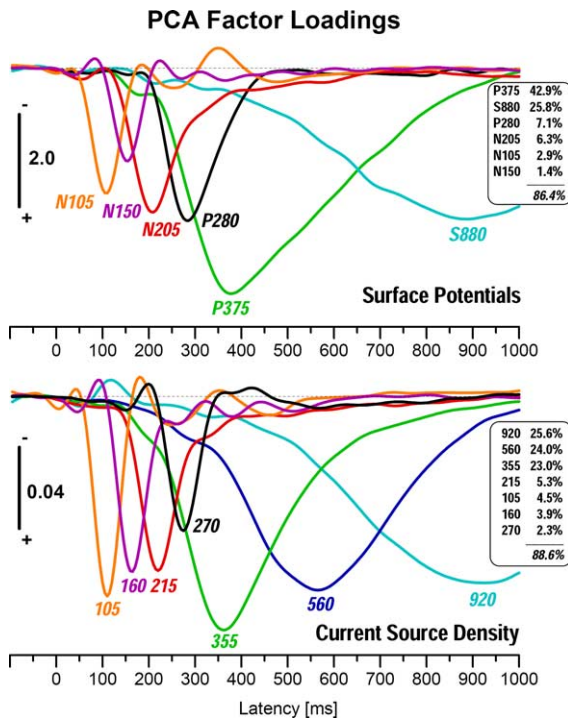


Fig. 4. Time courses of factor loadings for PCA components extracted from ERP (surface potentials; top) and CSD (current source density; bottom) waveforms. ERP and CSD factor labels indicate the peak latency of the factor loadings; for ERP factors, additional letters refer to the polarity of the corresponding ERP component (P: positive; N: negative; S: slow wave). Insets indicate the percentage of explained variance after Varimax rotation for each factor. (This figure appears in colour on the web).

exception of factor 560, which filled the transition between P3 (factors P375 and 355) and slow wave (S880 and 920). This observation is supported by the fact that the first two ERP factors (P375, S880) together accounted for almost the same variance (approximately 70%) as the first three CSD factors (920, 560, 355), suggesting that certain variance portions of factors S880 and particularly P375 of the time interval between approximately 450 and 700 ms were reallocated by the CSD transformation. It is also clear that the CSD solution produced factor loadings with less temporal overlap (i.e. ‘sharper’ time courses) compared with the ERP solution.

3.4. Component topographies of PCA solutions and statistical results

The factor score topographies of the PCA solutions derived from the ERP and CSD data sets are depicted in Fig. 5 for target stimuli in both tasks (averaged across response mode). To avoid redundancy, detailed descriptions of the factor score topographies are presented together with the report of their statistical results. Because of the close correspondence between ERP and CSD solutions, data are presented in a parallel fashion.

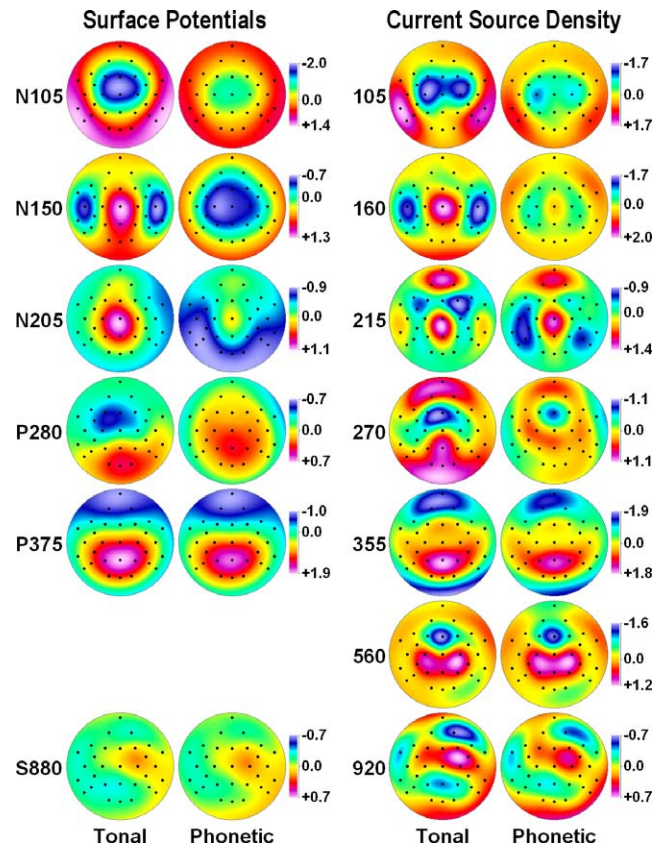


Fig. 5. Mean topographies of factor scores ($N=66$) for PCA components extracted from ERP (surface potentials; left) and CSD (current source density; right) waveforms. Topographies are shown for tonal (columns 1 and 3) and phonetic (columns 2 and 4) target stimuli only (averaged across response mode), and ordered from top to bottom according to the peak latency of the factor loadings. Black dots indicate the spherical positions of the 31-channel EEG montage (nose at top). All topographic maps are 2D-representations of spherical spline surface interpolations (Perrin et al., 1989; 1990; Appendix (Supplementary data, doi:10.1016/j.clinph.2005.08.034)) derived from the mean factors scores available for each recording site. (This figure appears in colour on the web).

3.4.1. Factors N105 and 105

Factor N105 (2.9% explained variance) overlapped N1 and had a negative amplitude at medial-central sites, particularly for the tonal task, which is entirely consistent with the central maximum of N1 and the task difference in N1 amplitude (Fig. 2). Similarly, factor 105 (4.5%) overlapped the central sink and the lateral temporo-parietal source peaking at 100 ms, and showed a corresponding negative amplitude over medial-central sites and a positive amplitude over lateral temporo-parietal sites. Statistical analyses for these two factors were restricted to medial-central sites (C3/4).

The ANOVA for ERP factor N105 revealed only one, however, highly significant task main effect, $F_{[1,64]}=47.8$, $P<.0001$. The ANOVA for CSD factor 105 also revealed a highly significant task main effect, $F_{[1,64]}=60.1$, $P<.0001$. Both of these effects supported the notion of greater N1 or sink amplitude in the tonal compared with the phonetic task (Fig. 5, row 1). In addition, a significant hemisphere main

effect, $F_{[1,64]}=7.36$, $P<.009$, was observed for CSD factor 105, stemming from a relative greater sink over the left than right hemisphere (Fig. 5).

3.4.2. Factors N150 and 160

Factor N150 (1.4%), the only ERP factor not considered in our previous reports, corresponded to the N1/P2 transition and had a negative amplitude, which was distinct at lateral-temporal sites in the tonal task, but broadly distributed across central sites in the phonetic task (Figs. 2 and 5, row 2). Similarly, factor 160 was characterized by a prominent lateral temporo-parietal sink for the tonal task, with a corresponding source maximal over vertex (Fig. 3; cf. Fig. 2 of Gomes et al., 2001). For syllables, factor 160 (3.9%) was like factor N150 markedly reduced in amplitude, however, its topography was comparable to the one observed for complex tones (Fig. 5, row 2). To adequately address these highly specific, task-dependent differences in factor score topographies, two separate ANOVA were computed for each of these two factors using either lateral-temporal sites (T7/8) or the mid-central site (Cz).

The statistical analyses at lateral-temporal sites revealed a highly significant task main effect for factor N150, $F_{[1,64]}=48.0$, $P<.0001$, and also for factor 160, $F_{[1,64]}=179.2$, $P<.0001$, thereby clearly confirming a greater negative amplitude and sink for tonal compared with phonetic stimuli. These task main effects were equally robust in the analyses at vertex (for factor N150, $F_{[1,64]}=94.5$; for factor 160, $F_{[1,64]}=180.6$, both $P<.0001$), confirming a greater positivity and source for tonal than phonetic stimuli. This task main effect was modulated for CSD factor 160 at lateral-temporal sites by a task \times hemisphere interaction, $F_{[1,64]}=9.21$, $p=.004$, stemming primarily from a right-greater-left-hemisphere sink in the tonal task (means were: at T7 = -1.72 , SD = 1.36; at T8 = -1.98 , SD = 1.34). Although comparable means were observed for the ERP factor N150, the task \times hemisphere interaction, $F_{[1,64]}=2.72$, $p=.10$, failed to reach statistical significance.

3.4.3. Factors N205 and 215

Factor N205 (6.3%) corresponded to N2 amplitude for targets, which overlapped a prominent P2 amplitude for frequent stimuli (Fig. 2). There was a marked task-dependent topography of this component, being greatest over right lateral fronto-temporal sites for tones, and over left lateral temporo-parietal sites for syllables (Fig. 5, row 3, left columns). This distinct task-dependent, asymmetric topography was even more evident in the CSD equivalent: factor 215 (5.3%) revealed distinct mid-frontal sinks for the tonal task, which were larger over the right hemisphere, whereas temporo-parietal sinks were found for the phonetic task, which were larger over the left hemisphere (Fig. 5, row 3, right columns). To capture the topographic specificity of these components, which implicated a task-dependent anterior-posterior gradient, two separate ANOVA were computed for each of these two factors, using five homologous pairs of either fronto-central (F3/4, F7/8,

FC5/6, C3/4, FT9/10) or centro-temporo-parietal (P7/8, P9/10, CP5/6, T7/8, TP9/10) sites in these analyses.

The analyses at anterior sites revealed a highly significant task main effect for ERP factor N205, $F_{[1,64]}=16.1$, $p=.0002$, and also for CSD factor 215, $F_{[1,64]}=29.9$, $P<.0001$, but these effects were opposite in nature. For the surface potentials, there was greater N2 amplitude for phonetic compared with tonal stimuli, whereas the anterior sink was greater for tonal than phonetic targets. However, the direction of the task \times hemisphere interaction, being larger over the right anterior sites for tones and larger over the left anterior sites for syllables, was alike and highly significant for factors N205, $F_{[1,64]}=32.7$, $P<.0001$, and 215, $F_{[1,64]}=13.1$, $p=.0006$. Significant simple hemisphere main effects were present for tones (right-larger-than-left) for ERP factor N205, $F_{[1,64]}=15.9$, $p=.0002$, and CSD factor 215, $F_{[1,64]}=10.5$, $p=.002$, but not syllables (left-larger-than-right; for N205, $F_{[1,64]}=2.38$, $p>.12$; for 215, $F_{[1,64]}<1.0$), indicating that the N2 asymmetry in the tonal task was the main source for the task \times hemisphere interaction over anterior regions.

The analyses at posterior sites also revealed highly significant task main effects for ERP factor N205, $F_{[1,64]}=33.3$, $P<.0001$, and CSD factor 215, $F_{[1,64]}=80.4$, $P<.0001$, and both originated from greater negativity in the phonetic than tonal task. A significant task \times hemisphere interaction was present for factor N205, $F_{[1,64]}=29.9$, $P<.0001$, stemming from opposite, significant N205 asymmetries for tones (right-larger-than-left, $F_{[1,64]}=8.08$, $P=.006$) and syllables (left-larger-than-right, $F_{[1,64]}=6.71$, $P=.01$). A similar task \times hemisphere interaction was found for factor 215, $F_{[1,64]}=4.41$, $P=.04$, but this interaction effect originated from an asymmetric posterior sink in the phonetic task only (left-larger-than-right, $F_{[1,64]}=9.77$, $P=.003$; for the tonal task, $F_{[1,64]}<1.0$).

In addition to task and hemisphere effects, these analyses for factors N205 and 215 revealed several effects involving response mode (Fig. 6). At anterior sites, a highly significant response mode \times hemisphere interaction was observed for N205, $F_{[2,128]}=11.0$, $P=.0001$, $\epsilon=.93$, and 215, $F_{[2,128]}=5.28$, $P=.007$, $\epsilon=.94$. For both factors, simple hemisphere main effects for each response mode indicated that the asymmetric right-larger-than-left negativity attained significance for left button presses only (for N205, $F_{[1,64]}=10.2$, $P=.002$; for 215, $F_{[1,64]}=8.78$, $P=.004$). At posterior sites, a highly significant response mode \times hemisphere interaction was also observed for N205, $F_{[2,128]}=14.1$, $P<.0001$, $\epsilon=.997$, but this interaction effect was clearly weaker for 215, $F_{[2,128]}=3.17$, $P<.05$, $\epsilon=.98$. The follow-up analyses revealed for factor N205 a significant simple hemisphere main effect (right-greater-than-left) for left button presses only ($F_{[1,64]}=5.20$, $P=.03$), whereas for factor 215 the opposite asymmetry (left-greater-than-right) was significant for right button presses only ($F_{[1,64]}=7.43$, $P=.008$). As no asymmetric amplitudes were found for silent count responses, these findings suggest that the

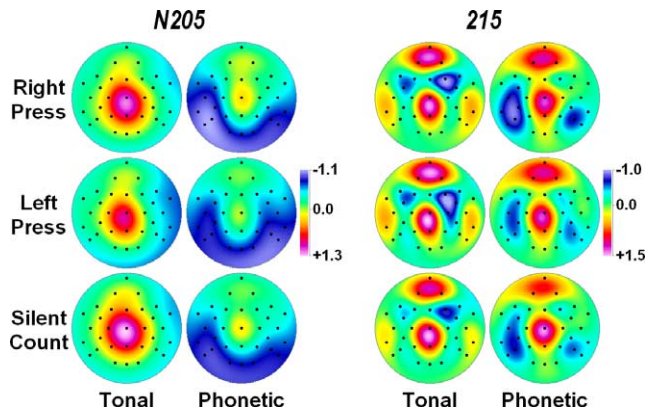


Fig. 6. Mean factor score topographies ($N=66$) for ERP factor N205 (left) and CSD factor 215 (right) for tonal (columns 1 and 3) and phonetic (columns 2 and 4) target stimuli and each response mode (rows 1–3). Recording sites (black dots) and map interpolations (2-D spherical spline) are indicated in Fig. 5. (This figure appears in colour on the web).

task-related regional asymmetries (i.e. anterior-right for tones, posterior-left for syllables) were either enhanced (tones) or reduced (syllables) with left button presses. This impression was further supported by a highly significant response mode \times task interaction, $F_{[2,128]}=7.13$, $P=.002$, $\epsilon=.89$, observed for CSD factor 215 in the analyses for posterior sites. Simple task main effects (phonetic-greater-than-tonal) were highly significant for all response modes (right press, $F_{[1,64]}=90.1$; left press, $F_{[1,64]}=32.0$; silent count, $F_{[1,64]}=36.1$, all $P<.0001$), however, clearly most robust for right button presses, which likely enhanced the left parietal sink during the phonetic task (Fig. 6).

3.4.4. Factors P280 and 270

At first glance, factor P280 (7.1%) appeared to correspond to the early phase of P3, given its time course and its posterior factor score positivity (Fig. 5, row 4, left columns). However, positive scores were shifted towards occipital sites for tones, but most prominent over mid-parietal sites for syllables, and a robust negativity over central sites was present for tones but not for syllables. Moreover, these P280 target topographies were very similar to the P280 topographies observed for frequent stimuli, which further challenges any P3-like interpretation of the factor. Instead, the CSD topographies for the associated factor 270 (2.3%) implicate a mid-central sink for either task, that is accompanied by an occipital source for the tonal task only (Fig. 5, row 4, right columns). These observations make it very difficult to unambiguously associate these topographies with a *known* ERP component for both tasks. Rather, we suspect that task-related and/or interindividual variance during the N2/P3 transition (latency jitter) contributed to the extraction of these factors. Because of these interpretational uncertainties and the resulting difficulty of selecting a representative subset of recording sites common to both tasks, no statistical analyses were

performed for these factors (cf. recommendations by Kayser and Tenke, 2003; see also Kayser and Tenke, 2006).

3.4.5. Factors P375 and 355

Factor P375 (42.9%) corresponded to a classical P3b amplitude for targets, having a wide parietal distribution with a Pz maximum in either task (Fig. 5, row 5, left columns). This posterior positivity coincided with an anterior negativity showing a Nose maximum. This dipole-like topography was somewhat more distinct for the associated CSD factor 355 (23.0%), which consisted of a prominent source spanning medial-parietal sites (Pz, P3/4, CP5/6) and a fronto-polar sink (Nose, Fp1/2; Fig. 5, row 5, right columns). As in our prior report (Kayser et al., 2001), three homologous pairs of medial and lateral centro-parietal sites (P3/4, CP5/6, P7/8) were selected for the ANOVA of these two factors.

A highly significant task \times hemisphere interaction was found for factors P375, $F_{[1,64]}=21.4$, $P<.0001$, and 355, $F_{[1,64]}=8.03$, $P=.006$. Simple hemisphere main effects revealed a significant left-greater-than-right P375 asymmetry for syllables ($F_{[1,64]}=14.6$, $P=.0003$) but not for tones ($F_{[1,64]}<1.0$), and a significant right-greater-than-left 355 asymmetry for tones ($F_{[1,64]}=4.16$, $P<.05$) but not for syllables ($F_{[1,64]}<1.0$). An overall left-greater-than-right hemisphere main effect was observed for the ERP factor P375, $F_{[1,64]}=5.35$, $P<.03$, but not for CSD factor 355.

A significant response mode \times hemisphere interaction, $F_{[2,128]}=15.1$, $P<.0001$, $\epsilon=.97$, was found for factor 355. A simple right-larger-than-left hemisphere main effect was found for left button presses, $F_{[1,64]}=10.8$, $p=.002$, but not for right press or silent count. As can be seen from target CSD topographies of factor 355 for each response mode (Fig. 7, right column), button presses produced a relative sink over contralateral motor regions (i.e. between sites Cz, C3, FC5, and F3, or Cz, C4, FC6, and F4), whereas such sinks were absent when participants silently counted targets. These response-related topographic effects are obviously less prominent in the surface potentials (cf. factor P375, Fig. 7, left column), although corresponding asymmetries for button presses can be detected after careful inspection.

3.4.6. Factor 560

The only CSD factor with no obvious ERP equivalent was factor 560 (24.0%), apparently sharing the larger ERP variance of factor P375 (42.9%) during this time range with CSD factor 355 (23.0%). The factor score topography for targets of factor 560 was characterized by a large, focal sink effectively restricted to site Fz, and two mid-central sources over somatosensory regions (Fig. 5, row 6). Two separate ANOVA were computed for factor 560, one employing only midline site Fz, the other using medial-central sites (C3/4).

The analysis of the mid-frontal sink revealed a highly significant response mode main effect, $F_{[2,128]}=5.58$, $P=.007$, $\epsilon=.89$. Across tasks, mean sinks were greater for button press than silent count responses (right press = -1.84 , $SD=1.38$; left press = -1.88 , $SD=1.53$; silent

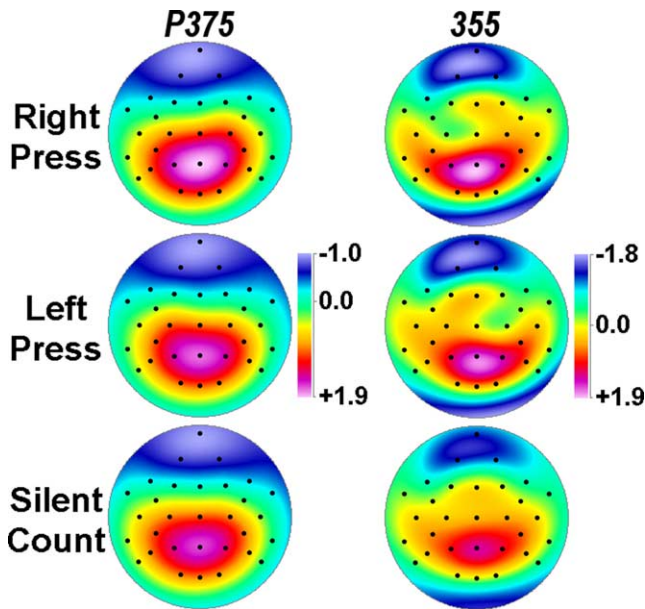


Fig. 7. Mean factor score topographies ($N=66$) for ERP factor P375 (left) and CSD factor 355 (right) for each response mode, averaged across tonal and phonetic target stimuli. Recording sites (black dots) and map interpolations (2-D spherical spline) are indicated in Fig. 5. (This figure appears in colour on the web).

count = -1.46 , $SD=1.47$), as confirmed by simple contrasts (right press vs. silent count, $F_{[1,64]}=7.52$, $P=.008$; left press vs. silent count, $F_{[1,64]}=6.84$, $P=.01$; right vs. left press, $F_{[1,64]}<1.0$).

A similar response mode main effect, $F_{[2,128]}=32.2$, $P<.0001$, $\epsilon=.81$, emerged in the analysis of the medial-central sources. Across tasks, mean sources were greater for button press than silent count responses (right press = 1.24 , $SD=1.37$; left press = 1.30 , $SD=1.29$; silent count = 0.51 , $SD=0.86$), as confirmed by simple contrasts (right press vs. silent count, $F_{[1,64]}=32.0$, $P<.0001$; left press vs. silent count, $F_{[1,64]}=47.0$, $P<.0001$; right vs. left press, $F_{[1,64]}<1.0$). This analysis also revealed a highly significant response mode \times hemisphere interaction, $F_{[2,128]}=8.16$, $P=.0008$, $\epsilon=.89$. Right button presses produced greater sources over right than left somatosensory regions ($F_{[1,64]}=8.94$, $P=.004$; Fig. 8, row 1). Although left button presses produced the opposite hemispheric asymmetry (i.e. greater sources over left than right somatosensory regions; Fig. 8, row 2), this effect lacked statistical support ($F_{[1,64]}<1.0$). A moderate right-larger-than-left 560 source asymmetry was present for silent count ($F_{[1,64]}=3.86$, $P=.05$; Fig. 8, row 3).

Fig. 8 (bottom row) also shows the net effect of detecting targets by either pressing a response button or by silently counting these stimuli (i.e. the mean 560 topography of left and right presses minus the 560 topography for silent count). As can be seen, these net differences are not restricted to the sink and source maxima (i.e. mid-frontal and medial-central regions), but were instead particularly evident over left temporal regions, which showed considerable source activity for the silent count condition. Another post-hoc ANOVA was therefore computed for factor 560 using three

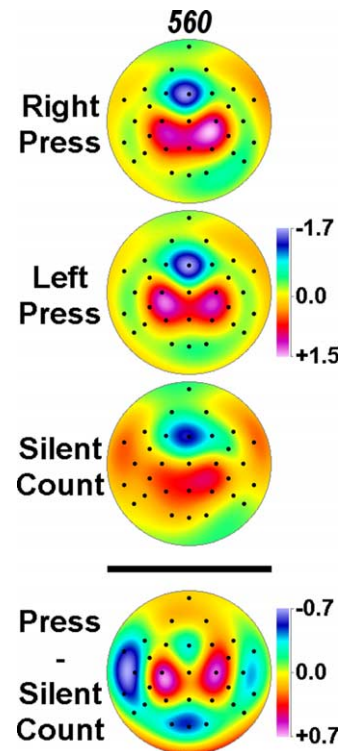


Fig. 8. Mean factor score topographies ($N=66$) for CSD factor 560 for each response mode, averaged across tonal and phonetic target stimuli, and the topographic difference of button press (average of right and left press) minus silent count responses. A symmetric scale was applied to the difference topography. Recording sites (black dots) and map interpolations (2-D spherical spline) are indicated in Fig. 5. (This figure appears in colour on the web).

homologous pairs of lateral-temporal sites (FT9/10, T7/8, TP9/10). This analysis confirmed the greater 560 source at temporal sites for silent count versus button press responses (response mode main effect, $F_{[2,128]}=21.9$, $P<.0001$, $\epsilon=.81$; simple contrasts, right press vs. silent count, $F_{[1,64]}=33.3$, left press vs. silent count, $F_{[1,64]}=29.1$, both $P<.0001$; right vs. left press, $F_{[1,64]}<1.0$), as well as the left-greater-than-right source asymmetry for silent count only (response mode \times hemisphere interaction, $F_{[2,128]}=5.67$, $P=.005$, $\epsilon=.93$; simple hemisphere main effect at silent count, $F_{[1,64]}=4.81$, $p=.03$).

3.4.7. Factors S880 and 920

Since no known ERP component topography could be associated with the topographic patterns of the two late ERP and CSD factors (Fig. 5, row 7), thereby rendering these factors likely candidates of unsystematic, spurious ERP variance contributions at the end of the recording epoch (e.g. Kayser and Tenke, 2003; van Boxtel, 1998), no further statistical analyses were performed for these factors (see also Kayser and Tenke, 2006).

4. Discussion

The current study evaluated reference-free CSD transformations of ERP surface potentials as an intermediate

processing step to further improve the PCA-ERP analytic approach (e.g. Chapman and McCrary, 1995), building on the benefits of using unrestricted, covariance-based, temporal PCA with Varimax rotation (Kayser and Tenke, 2003). Since this evaluation was based on a parallel analysis of CSD/ERP data obtained from tonal and phonetic oddball paradigms known to produce distinct effects of stimulus type and response mode, the effectiveness of these two approaches will be discussed first. The analyses of these real auditory oddball ERPs served as a prototype of this new and possibly more generic analytic strategy. The inclusion of silent count as a response mode condition, in addition to left and right button press, and the completely within-subjects design, provided an excellent new opportunity to dissociate topographic specificity associated with task and response mode using this new tool.

As expected, the PCA factor structure derived from the surface potential ERP data closely matched those previously reported for tonal and phonetic oddball tasks (Kayser et al., 1998, 2000b, 2001), yielding factors corresponding to N1, P2/N2, P3 and slow wave, thereby supporting the validity of intended comparisons to our prior studies. As before, task-related, region-specific hemispheric asymmetries were observed for target ERP components (i.e. N2 and P3), showing larger amplitudes over the right hemisphere for tones, and larger amplitudes over the left hemisphere for syllables. Likewise, task-related asymmetries were modulated by superimposed, response-related asymmetries, primarily affecting components of the N2/P3 complex. The findings from the new approach using CSD instead of ERP waveforms helped to clarify and separate these complex contributions of task and response mode.

4.1. Similarities and differences of ERP and CSD solutions

PCA solutions based on CSD averages resulted in similar factors derived from ERP waveforms. However, there was less temporal overlap (i.e. ‘sharper’ time courses) for CSD factor loadings when compared with the ERP solution, and factor score topographies were generally more sharply differentiated. For some ERP components, the topographies of corresponding factor scores were remarkably similar for ERP and CSD solutions. For example, the topographies of factors representing N1 (N105/105) were quite similar for the tonal task, differing primarily in a better separation of frontocentral sinks from the midline and modality-specific dipolar alignment along the Sylvian fissure for the CSD solution, with corresponding sources being better confined to the temporal lobe.² The factor score topographies for the phonetic task were similar, but smaller in amplitude,

and this similarity was not immediately evident from the ERP solution. The topographic enhancement of the CSD solution also revealed the presence of a left-greater-than-right N1 sink, which is consistent with our observations of statistically-insignificant asymmetric N100 peaks in the grand mean ERP waveforms (Kayser et al., 1998; 2001). Asymmetrical temporal lobe distributions of N1m sources, the neuromagnetic equivalent to the N1 component, have been reported (e.g. Zouridakis et al., 1998), and these dipole locations are affected by stimulus properties (e.g. duration; Rosburg et al., 2002). It is likely that the marked anatomical asymmetry of central sulcus and temporal lobe (Heschl’s gyrus, planum temporale) in the left and right hemisphere provide asymmetric contributions to N1 (Ohtomo et al., 1998; Witelson and Kigar, 1988).

For the factor representing temporal N1 (N150/160), the corresponding topographies were also similar for the two solutions, with a midline positivity/source being more sharply confined to Cz for the CSD solution. Although the negativity in the ERP solution was widely distributed across the central and medial scalp for the phonetic task, the CSD sink topography spanned from frontal to temporal sites, yet excluded Cz. Thus, the CSD activation pattern was quite similar to tones but smaller in amplitude, which was again not apparent from the ERP solution. The dynamic temporal-spatial linkage between central N1 and temporal N1 becomes quite obvious from the animated topographies, implicating an N1 dipole rotation using the Sylvian fissure as axis. Nevertheless, the two factors associated with central N1 and temporal N1 provide an effective summary of this ERP progression. The CSD solution revealed a robust interaction of task and hemisphere, suggesting a stronger right-than-left temporal N1 activation for tones, thereby preceding tonal N2 effects. However, it should be noted that the present active oddball paradigm is inadequate to distinguish between overlapping early negativities, which may also involve asymmetric mismatch negativities previously observed for tonal and phonetic stimuli (Aaltonen et al., 1993; Alho et al., 1996; Giard et al., 1990; Näätänen, 1990; Shtyrov et al., 2000).

For the factor representing N2 (N205/215), the CSD solution greatly simplified the distinct task-related N2 asymmetries, by unambiguously separating posterior (parietal-temporal) sinks in the phonetic task from anterior (frontal-central) sinks in the tonal task, and revealing marked, opposite sink asymmetries resulting from the engagement of predominantly left or right hemisphere functions for phoneme and pitch discrimination. Task-related asymmetries also prevailed for the factor representing P3b (P375/355), which was characterized a typical mid-parietal positivity opposite a mid-anterior negativity common to both ERP and CSD solutions, but sharper and better focused in the latter. The overall, volume-conducted left hemisphere shift in the ERP surface potentials, which likely contributed to the phonetic left-larger-than-right P3b amplitude, was eliminated by the CSD transformation,

² An auditory N1 is a special case in that the nose functions as an ‘inactive’ reference by virtue of being located along a line that is approximately perpendicular to the surface lamination of modality-specific cortex within the Sylvian fissure. In contrast, a linked mastoid or ear reference would significantly distort the raw field N1 topography.

revealing instead a tonal right-larger-than-left P3b amplitude. These findings and their interpretations are in remarkable agreement with previous electrophysiologic (e.g. Celsis et al., 1999; Kayser et al., 1998; 2001; Maiste et al., 1995; Wioland et al., 1999), neuroimaging (e.g. Belin et al., 1998; 2002; Zatorre et al., 1992), and neurological (e.g. Zatorre, 1988; 2001) evidence (see Hickok and Poeppel, 2004, for a recent theoretical framework).

The overlap of stimulus-locked ERP components and movement-related potentials, consisting of a series of slow and fast negative and positive deflections preceding and following the actual motor act (e.g. Hillyard and Picton, 1987), are a well-known problem in ERP research (e.g. Kok, 1988). For both N2 and P3b, which uniquely emerge during the response-related target conditions in these auditory oddball tasks, the CSD compared with the ERP solution simplified and clarified the origin of topographic effects related to response mode, involving pre- and postcentral generators of the sensorimotor cortex, as well as supplementary, premotor, and prefrontal cortex (e.g. Singh and Knight, 1990). Sink activity at medial-central sites contralateral to the response hand used for the button press, which clearly preceded motor responses largely occurring between 400 and 600 ms, resulted in a relative contralateral N2 enhancement for manual responses only. Likewise, button press resulted in a relative P3b reduction over medial-central sites contralateral to the response hand, notably displaced from the P3b maximum over mid-parietal sites. While the ERP surface potentials replicate and extend the right press and silent count findings of Salisbury et al. (2001, 2004), these P3 asymmetries and their premotor origin are unambiguously identified and separated by the CSD solution. Unlike previous studies using a linked ear lobe reference (Barrett et al., 1987; Salisbury et al., 2001), we found no evidence that button pressing reduces P3b amplitude when using nose-referenced ERPs or reference-free CSDs. Rather, the present results are more in agreement with the finding that right-hand responses contribute to right-hemispheric P3 source activation in right-handers (Tenke et al., 1998).

Despite the comparability of the ERP and CSD factor score topographies for P3b, the CSD solution provided additional clarification of the late positive complex by identification of a subcomponent following P3b. The separation of ERP factor P375, which reveals the typical characteristics of a classical P3b component (e.g. Fabiani et al., 2000; Sutton et al., 1965), into CSD factors 355 and 560 is a completely new finding.³ It is one of the

pitfalls of a temporal PCA that multiple ERP components completely overlapping in time are not separated, but rather extracted as a single factor, causing interpretational difficulties (cf. P3/N3 factors described in Kayser et al., 1997; 1998). The present result suggests that spatial CSD enhancement is capable of separating unique variance contributions presumably caused by overlapping movement-related potentials from the time-locked variance associated with a classical P3b. The topography of this late CSD factor includes a distinctive, focal mid-frontal sink in both tasks, associated with source activity in centroparietal (somatosensory) regions. Although both topographic features (Fz sink, centroparietal source) were observed across all three response conditions, both sink and source amplitudes were markedly enhanced for button press compared to silent count. Moreover, the centroparietal sources also revealed a robust button press asymmetry favoring the hemisphere ipsilateral to the response hand, particularly for right-hand presses, which matches our previous finding based on an integrated time window also showing a lateralization of late (430–700 ms) P3 source activity ipsilaterally to the response hand (Tenke et al., 1998). Consistently, response-locked surface Laplacians recorded over primary motor areas showed that contralateral sink activity is accompanied by source activity ipsilateral to response hand (Carbonnell et al., 2004; Vidal et al., 2003).

Interestingly, button pressing and mental counting produced separable intracranial P3-like potentials during a somatosensory oddball paradigm in epileptic patients in addition to P3-like potentials not systematically associated with either response mode (Brazdil et al., 2003). This, together with more recent findings using a visual oddball task (Roman et al., 2005), strongly suggests multiple, independent P3 generators in middle and inferior lateral temporal cortex, anterior cingulate, and orbitofrontal and dorsolateral prefrontal cortex (see also Brazdil et al., 2005; Halgren et al., 1995a; 1995b; Knight et al., 1989), which can be partially distinguished by their association with stimulus and/or response. Given the topographic pattern and temporal sequence of our findings, we hypothesize that the centroparietal source summarized in CSD factor 560 largely reflects response-related P3 source activity, whereas the parietal source summarized in CSD factor 355 largely reflects stimulus-related P3 source activity.

The focal mid-frontal sink is of particular interest, as its topography suggests a relationship to the error-related negativity (ERN/Ne), which is observed over the centromedial cortex when individuals become aware of having committed an error, and which has more recently been interpreted as an electrophysiological correlate of action monitoring and regulation involving the anterior cingulate and supplemental motor areas (e.g. Luu et al., 2000; Luu and Tucker, 2001; Luu et al., 2003; Luu

³ The selection of physiologically-relevant ERP and CSD factors is entirely consistent with criteria developed in our previous work using ERPs (Kayser et al., 1998; 2001; Kayser and Tenke, 2003). Moreover, the decision to consider CSD factor 560, but not factors S880 and 920, for example, was further vindicated by the extended correlation analyses presented in our accompanying report (Kayser and Tenke, 2006), which evaluated the comparability of high and low resolution CSD factor scores for individual topographies.

et al., 2004).⁴ In healthy adults, the ERN may also be found during correct trials (Gehring and Knight, 2000; Vidal et al., 2000). Two recent response-locked surface Laplacian studies observed a distinct FCz sink that preceded the motor response, suggesting it reflects response selection and/or programming by the supplementary motor area (Carbonnell et al., 2004; Vidal et al., 2003). Interestingly, the mid-frontal sink reported here was also observed in a condition requiring no overt motor response. Although speculative, we propose that the mid-frontal sink summarized in CSD factor 560 reflects motivational response selection or evaluation, which is also present when mentally counting targets, however, less pronounced as compared to overt motor responses. It will be an interesting challenge to employ this new ERP-CSD-PCA approach in a combination of oddballs tasks and more appropriate ERN designs (e.g. conflict, Go-NoGo, and Stroop tasks) to test this hypothesis, and when using a response-locked analysis, all of which is beyond the scope of this paper.

Finally, the late CSD factor revealed a left-lateralized P3 source spanning fronto-temporal-parietal regions for the silent count condition only, which was not immediately evident from the ERP solution or the raw ERPs. We interpret this late P3 source as an electrophysiological correlate of updating, memorizing, or rehearsing the mental count, which is presumably mediated by language-related and/or serial processing resources, which primarily involve left-hemispheric functions (e.g. Hickok and Poeppel, 2004).

4.2. Improving the ERP-PCA approach through CSD transformation

For ERP surface potentials, a temporal PCA provides a concise, statistical description of the waveform variance (e.g. Chapman and McCrary, 1995; Donchin and Heffley, 1978; Kayser and Tenke, 2003). For multichannel ERPs, these waveforms are necessarily intercorrelated due to synchronized activity and redundancy introduced by volume conduction. To the extent that ERP superposition at the scalp conforms to a linear model, the solutions produced by PCA are likely to identify physiologically meaningful components. The usefulness of PCA is therefore largely a byproduct of the linear mathematical model on

which it is based: PCA identifies common linear factors within an ERP dataset, such as the contributions from functionally and anatomically distinct, but concurrent, neuronal generators, even in the absence of condition and subject variance.

There are three distinct sources of variance that affect the component shapes (factor loadings) and topographies (factor scores) identified by PCA: variation across electrodes, across experimental conditions, and across subjects (including groups). Of these, electrode variance is most closely related to the classical definition of an ERP component—CSD as a spatial transformation (i.e. second spatial derivative) affects only this variance source by detecting and emphasizing edges and discontinuities in the topography, effectively simplifying the overall ERP variance. For instance, the finer spatial structure of N1 (e.g. closer alignment to the Sylvian fissure) for the CSD than the ERP solution, or the better differentiation and improved consistency of N2 (affording easier interpretation of conditions), are a direct consequence of removing spatial redundancy caused by volume conduction through the brain and skull. On the other hand, the common linear geometry of CSD and PCA, which are based on quite different theoretical models and algorithms, may account for the remarkable similarity between ERP- and CSD-based PCA solutions, underscoring the value of CSD transformation as a generic preprocessing step for PCA.

By removing linear, volume-conducted signal contributions from distant recording sites, CSD completely eliminates the variance related to the recording reference for ERP surface potentials, that is, arbitrary signal variance introduced by the reference choice. While the second spatial derivative will also eliminate the contributions of deep generators, such common activity will only be measured by referenced ERPs if the reference is differentially affected. Otherwise, it is already eliminated during the ERP acquisition process. Despite the theoretical possibility that generators of intermediate depth may affect only a subset of the EEG montage, and that such activity, as well as activity transmitted across the cortex by wave propagation (e.g. Robinson, 2003), will then be underestimated by the CSD transformation, we found no evidence of this in our data, which must be considered a prototypical ERP paradigm. Rather than obscuring the ERP component structure (e.g. missing a component), all critical ERP components were preserved after CSD transformation with improved representation, and, moreover, an additional, meaningful component emerged. Thus, by also using a CSD transformation, we gained rather than lost information.

The average reference has been recommended as a means of decreasing the reference-dependence of a scalp topography (e.g. Dien, 1998b; Pascual-Marqui and Lehmann, 1993), and has the mathematical advantage of treating the reference identically to all other electrodes in the montage. However, an average reference is montage-specific, particularly when the montage is sparse, and has

⁴ The interpretation of the origin of sharply localized activity along the midline requires considerable caution, since a midline focus in a CSD topography is inconsistent with the placement of a single, radially-projecting dipole or dipole pair within the longitudinal fissure. No plausible mechanism exists for activating the laminae of cortex in a tangential pattern necessary to produce a consistent focal activity. Instead, activity should be oriented orthogonally to the cortical surface. Therefore, the focal mid-frontal sink indicates considerable field closure and cancellation at the surface, its topography is consistent with an activation pattern that includes bilateral regional dipoles located in the walls of the medial surface with opposite orientations perpendicular to the midsagittal plane (see Tenke et al., 1993, for a simulation of field closure in an intracranial CSD profile).

the practical limitation of reducing or excluding field contributions from the ventral surface of the braincase, and introducing a bias to the center of EEG montage, which is typically the vertex pole (Junghöfer et al., 1999). Although the accuracy of the CSD transformation is also montage-specific, largely affecting the undersampled edges of the EEG montage, and depends on the specific geometric model used (Hjorth, 1975; 1980; Perrin et al., 1989; Tenke et al., 1998; Tandonnet et al., 2005; Yao, 2002a), CSD nonetheless completely removes the impact of the recording reference (i.e. it is a reference-free transformation), whereas the average reference just replaces the recording reference with a different reference. Conversely, CSD measures are no longer protected by the inherent signal redundancy of ERP surface potentials, and are therefore subject to noise caused by electrode location errors, and computational noise resulting from a reliance on small, local differences (e.g. Srinivasan et al., 1996; Junghöfer et al., 1997). While these computational problems may be exacerbated with a low- or medium-density EEG montage, particularly on an individual basis, it appears that a low-resolution CSD may be entirely adequate to satisfactorily differentiate sink and source activity (e.g. Babiloni et al., 2001; Cincotti et al., 2004; Foffani et al., 2004; Tenke et al., 1993), and these problems were notably not evident in the present findings based on a very large sample. In fact, we have shown in an accompanying report that low-density surface Laplacian estimates based on our 31-channel 10–20 system EEG montage are accurate approximations of high-density CSDs for the auditory, three-response-mode oddball paradigm used in the present report, and that these low-density CSDs adequately and sufficiently summarized group data (Kayser and Tenke, 2006).

In view of the spatial origin of much of the observed variation in (temporal) ERP waveforms, and the importance of topography for defining an ERP component, it could be argued that spatial variance is more important than temporal variance to identify physiologically meaningful components, consequently using a spatial PCA as a preprocessing step for a temporal PCA to identify ‘virtual electrodes’ (Spencer et al., 1999; 2001). While this new spatiotemporal PCA has convincingly demonstrated its discriminative power by differentiating a classical P300 from a novelty P3, the topographies of the resulting spatiotemporal component constitute an entity that can only be compared with respect to conditions (including groups), but not with respect to the spatial configuration itself. Conventional statistical comparisons of activity across homologous electrodes over the two hemispheres, or any other regional comparisons (e.g. anterior versus posterior), can no longer be performed, however, these may not always be relevant to the research objective. In contrast, a temporal PCA allows statistical comparisons between any electrode sites included in the montage, which are preserved by the CSD transformation, with the additional advantage of having a simplified spatial structure and a concrete physiological

relevance. Of course, a spatial PCA can also readily be applied to CSD waveforms, and such an analysis has the potential of providing yet another perspective on the organization of ERP variance.

4.3. Validation of the suggested CSD-PCA approach

An open question that emerged during the review process was how can one know for sure which of the two considered solutions (i.e. ERP-PCA or CSD-PCA) summarized the data better, and how could one validate their appropriateness? By itself, a covariance-based PCA, followed by unrestricted Varimax rotation of covariance loadings provides a concise summary of the variance structure of the underlying data, regardless of its meaning (Kayser and Tenke, 2003); therefore, both solutions are valid and efficient summaries of the given data. It follows that the validation issue must rest on attributes of the submitted data. In this case, CSD removes spatial redundancy, is reference-independent, and provides information about the underlying neuronal generators, all of which has substantial practical implications. Assuming that both ERP-PCA and CSD-PCA solutions produced comparable outcomes, the latter one is better by definition. Different reference schemes (e.g. nose, linked mastoids, average reference) will produce different ERP-PCA solutions, but all will result in the same unique PCA solution after CSD transformation, which is not a mere theoretical advantage. Since CSD factors were as interpretable as ERP factors, and were also found to be superior in fulfilling all three criteria to qualify as a component (i.e. distinct time course, distinct topography, sensitivity to experimental manipulation; cf. Kayser and Tenke, 2003, 2005; Picton et al., 2000), it is concluded that CSD-PCA is the more valid approach.

One could also argue that a simulation study using a known set of equivalent current dipoles could provide a basis for validating and comparing the patterns of activation identified by ERP or CSD factors. While the insights gained by more or less arbitrarily modeling component prototypes may be useful, they are necessarily limited in scope and can never account for the complexity of generators underlying real ERP components. However, the value of a simulation study for the purpose of deciding which solution is better remains unclear, as any possible outcome cannot be generalized to all real ERP components and/or studies. Likewise, the quest is to decide which solution is universally more valuable for simplifying and understanding the empirical data at hand, rather than trying to identify which one better approximates the number and configuration of simulated dipoles.

Finally, one might advocate using external measures of brain activation, such as positron emission tomography (PET) or functional magnetic resonance imaging (fMRI), to cross-validate patterns of activation identified by ERP or CSD factors. Unfortunately, neither hemodynamic or metabolic measures are appropriate to provide a standard

for transient electrophysiologic or neuromagnetic measures, because of their completely different time scale and the indirect manner by which they measure neuronal function and activity (e.g. Nunez and Silberstein, 2000). Rather, neuroimaging and electrophysiologic measures complement each other. It is one of the exciting frontiers in neuroscience to determine any correspondence between specific ERP components and common neuroimaging measures (e.g. Brazdil et al., 2005; Logothetis et al., 2001).

4.4. Conclusions

CSD transformation proved to be a valuable preprocessing step for PCA of ERP data, providing a unique, physiologically meaningful solution to the ubiquitous reference problem, while simplifying and reducing the redundancy of ERP topographies. Exemplified by the findings for tonal and phonetic oddball data, the composite CSD-PCA approach resulted in very similar factors to those produced using a conventional ERP-PCA, confirming previous conclusions about task- and response-related component topographies and asymmetries. For instance, the topography of N2 for the phonetic task was topographically distinguishable from tonal N2 based on topographic criteria (i.e. more posterior; greater over left than right hemisphere), which is consistent with previous findings.

Similarly, response-related ERP asymmetries were replicated as expected, and their underlying generator patterns were clarified using CSD-PCA, including those for silent count as a response mode. P3-related activity favored the hemisphere ipsilateral to the response hand, particularly for right-hand presses. Unlike ERP-PCA, the CSD-PCA solution distinguished stimulus-related and response-related P3 activity by identifying an additional subcomponent of the late positive complex following P3b, which was observed for both tasks and all three response modes: a distinctive, focal, mid-frontal sink associated with a centroparietal source. This late, response-related P3 subcomponent was not only greater ipsilateral to the response hand (i.e. asymmetric for manual responses), but also differentiated silent count from motor responses by an asymmetric, left temporal source enhancement.

Overall, the CSD-PCA solution revealed sharper topographies when compared to ERP-PCA, but no ERP effects of interest were distorted or lost. Instead, new insights into well-studied and traditionally accepted ERP constructs were obtained. By using a physiologically meaningful transformation that eliminates any ambiguities stemming from the recording reference, CSD provides a bridge between montage-dependent scalp potentials and their underlying current generators. The resulting reference-free waveforms are effectively summarized by means of unrestricted, covariance-based temporal PCA. The similarity of the ERP- and CSD-PCA factor structures suggests that the two approaches provide indices of the same or at least closely-

related phenomena. The advantages of CSD can, therefore, be readily exploited in typical research applications using groups of individuals. For these reasons, the combined CSD-PCA approach shows promise as a comprehensive, generic strategy for ERP analysis.

Acknowledgements

This research was supported by grants MH058346, MH36295, MH50715, and MH59342 from the National Institute of Mental Health (NIMH).

We greatly appreciate the assistance of Nil Bhattacharya, Carlye Griggs, Paul Leite, Mia Sage, Stewart Shankman, and Barbara Stuart with data collection, storage, and preprocessing.

Waveform plotting software was written by Charles L. Brown, III, who also provided helpful insights during the implementation of the spherical spline algorithm, benefiting from gracious advice given earlier by Patrick Berg. Thanks is also due to Robert Oostenveld for discussing options of modeling electrode locations on the head surface.

Supplementary data

Supplementary data associated with this article can be found at [doi:10.1016/j.clinph.2005.08.034](https://doi.org/10.1016/j.clinph.2005.08.034)

References

- Aaltonen O, Tuomainen J, Laine M, Niemi P. Cortical differences in tonal versus vowel processing as revealed by an ERP component called mismatch negativity (MMN). *Brain Lang* 1993;44(2):139–52.
- Achim A, Marcantoni W. Principal component analysis of event-related potentials: misallocation of variance revisited. *Psychophysiology* 1997; 34(5):597–606.
- Alho K, Tervaniemi M, Huottilainen M, Lavikainen J, Tiitinen H, Ilmoniemi RJ, Knuutila J, Näätänen R. Processing of complex sounds in the human auditory cortex as revealed by magnetic brain responses. *Psychophysiology* 1996;33(4):369–75.
- Babiloni F, Cincotti F, Bianchi L, Pirri G, del R Millan J, Mourino J, Salinari S, Marciani MG. Recognition of imagined hand movements with low resolution surface Laplacian and linear classifiers. *Med Eng Phys* 2001;23(5):323–8.
- Barrett G, Neshige R, Shibasaki H. Human auditory and somatosensory event-related potentials: effects of response condition and age. *Electroencephalogr Clin Neurophysiol* 1987;66(4):409–19.
- Beauducel A, Debener S. Misallocation of variance in event-related potentials: simulation studies on the effects of test power, topography, and baseline-to-peak versus principal component quantifications. *J Neurosci Methods* 2003;124(1):103–12.
- Beauducel A, Debener S, Brocke B, Kayser J. On the reliability of augmenting/reducing: peak amplitudes and principal components analysis of auditory evoked potentials. *J Psychophysiol* 2000;14(4): 226–40.

- Belin P, Zilbovicius M, Crozier S, Thivard L, Fontaine A, Masure MC, Samson Y. Lateralization of speech and auditory temporal processing. *J Cogn Neurosci* 1998;10(4):536–40.
- Belin P, McAdams S, Thivard L, Smith B, Savel S, Zilbovicius M, Samson S, Samson Y. The neuroanatomical substrate of sound duration discrimination. *Neuropsychologia* 2002;40(12):1956–64.
- Berlin CI, Hughes LF, Lowe Bell SS, Berlin HL. Dichotic right ear advantage in children 5 to 13. *Cortex* 1973;9(4):394–402.
- Brazdil M, Roman R, Daniel P, Rektor I. Intracerebral somatosensory event-related potentials: effect of response type (button pressing versus mental counting) on P3-like potentials within the human brain. *Clin Neurophysiol* 2003;114(8):1489–96.
- Brazdil M, Dobsik M, Mikl M, Hlustik P, Daniel P, Pazourkova M, Krupa P, Rektor I. Combined event-related fMRI and intracerebral ERP study of an auditory oddball task. *Neuroimage* 2005;26(1):285–93.
- Bruder GE. Cerebral laterality and psychopathology: perceptual and event-related potential asymmetries in affective and schizophrenic disorders. In: Davidson RJ, Hugdahl K, editors. *Brain asymmetry*. Cambridge, MA: MIT Press; 1995. p. 661–91.
- Bruder GE, Kayser J, Tenke CE, Leite P, Schneier FR, Stewart JW, Quitkin FM. Cognitive ERPs in depressive and anxiety disorders during tonal and phonetic oddball tasks. *Clin Electroencephalogr* 2002;33(3):119–24.
- Buzsaki G, Czopf J, Kondakor I, Kellenyi L. Laminar distribution of hippocampal rhythmic slow activity (RSA) in the behaving rat: current-source density analysis, effects of urethane and atropine. *Brain Res* 1986;365(1):125–37.
- Carbannel L, Hasbroucq T, Grapperon J, Vidal F. Response selection and motor areas: a behavioural and electrophysiological study. *Clin Neurophysiol* 2004;115(9):2164–74.
- Casarotto S, Bianchi AM, Cerutti S, Chiarenza GA. Principal component analysis for reduction of ocular artefacts in event-related potentials of normal and dyslexic children. *Clin Neurophysiol* 2004;115(3):609–19.
- Cattell RB. Screen test for number of factors. *Multivar Behav Res* 1966;1(2):245–76.
- Celsis P, Doyon B, Boulanouar K, Pastor J, Demonet JF, Nespoulous JL. ERP correlates of phoneme perception in speech and sound contexts. *NeuroReport* 1999;10(7):1523–7.
- Chapman RM, McCrary JW. EP component identification and measurement by principal components analysis. *Brain Cogn* 1995;27(3):288–310.
- Cincotti F, Babiloni C, Miniussi C, Carducci F, Moretti D, Salinari S, Pascual-Marqui R, Rossini PM, Babiloni F. EEG deblurring techniques in a clinical context. *Methods Inf Med* 2004;43(1):114–7.
- Desmedt JE, Tomberg C. Topographic analysis in brain mapping can be compromised by the average reference. *Brain Topogr* 1990;3(1):35–42.
- Dien J. Addressing misallocation of variance in principal components analysis of event-related potentials. *Brain Topogr* 1998a;11(1):43–55.
- Dien J. Issues in the application of the average reference: review, critiques, and recommendations. *Behav Res Methods Instrum Comput* 1998b;30(1):34–43.
- Dixon WJ, editor. *BMDP statistical software manual: to accompany the 7.0 software release*. Berkeley, CA: University of California Press; 1992.
- Donchin E. A multivariate approach to the analysis of average evoked potentials. *IEEE Trans Biomed Eng* 1966;13(3):131–9.
- Donchin E, Heffley EF. Multivariate analysis of event-related potential data: a tutorial review. In: Otto DA, editor. *Multidisciplinary perspectives in event-related brain potential research*. Proceedings of the fourth international congress on event-related slow potentials of the brain (EPIC IV), Hendersonville, NC, April 4–10, 1976. Washington, DC: The Office; 1978. p. 555–72.
- Donchin E, Ritter W, McCallum WC. Cognitive psychophysiology: the endogenous components of the ERP. In: Callaway E, Tueting P, Koslow SH, editors. *Event-related brain potentials in man*. New York: Academic Press; 1978. p. 349–411.
- Fabiani M, Gratton G, Coles MGH. Event-related brain potentials: methods, theory, and applications. In: Cacioppo JT, Tassinari LG, Bernston GG, editors. *Handbook of psychophysiology*. 2nd ed. New York: Cambridge University Press; 2000. p. 53–84.
- Fallgatter AJ, Strik WK. The NoGo-anteriorization as a neurophysiological standard-index for cognitive response control. *Int J Psychophysiol* 1999;32(3):233–8.
- Fallgatter AJ, Eisenack SS, Neuhauser B, Aranda D, Scheuerpflug P, Herrmann MJ. Stability of late event-related potentials: topographical descriptors of motor control compared with the P300 amplitude. *Brain Topogr* 2000;12(4):255–61.
- Foffani G, Bianchi AM, Cincotti F, Babiloni C, Carducci F, Babiloni F, Rossini PM, Cerutti S. Independent component analysis compared to laplacian filtering as ‘Deblurring’ techniques for event related desynchronization/synchronization. *Methods Inf Med* 2004;43(1):74–8.
- Friedman A, Polson MC. Hemispheres as independent resource systems: limited-capacity processing and cerebral specialization. *J Exp Psychol Hum Percept Perform* 1981;7:1031–58.
- Gehring WJ, Knight RT. Prefrontal–cingulate interactions in action monitoring. *Nat Neurosci* 2000;3(5):516–20.
- Gevens A. The future of electroencephalography in assessing neurocognitive functioning. *Electroencephalogr Clin Neurophysiol* 1998;106(2):165–72.
- Gevens A, Cutillo B, Smith ME. Regional modulation of high resolution evoked potentials during verbal and non-verbal matching tasks. *Electroencephalogr Clin Neurophysiol* 1995;94:129–47.
- Giard MH, Perrin F, Pernier J, Bouchet P. Brain generators implicated in the processing of auditory stimulus deviance: a topographic event-related potential study. *Psychophysiology* 1990;27(6):627–40.
- Glaser EM, Ruchkin DS. *Principles of neurobiological signal analysis*. New York: Academic Press; 1976.
- Gomes H, Dunn M, Ritter W, Kurtzberg D, Brattson A, Kreuzer JA, Vaughan Jr HG. Spatiotemporal maturation of the central and lateral N1 components to tones. *Brain Res Dev Brain Res* 2001;129(2):147–55.
- Halgren E, Baudena P, Clarke JM, Heit G, Liegeois C, Chauvel P, Musolino A. Intracerebral potentials to rare target and distractor auditory and visual stimuli. I. Superior temporal plane and parietal lobe. *Electroencephalogr Clin Neurophysiol* 1995a;94(3):191–220.
- Halgren E, Baudena P, Clarke JM, Heit G, Marinkovic K, Devaux B, Vignal JP, Biraben A. Intracerebral potentials to rare target and distractor auditory and visual stimuli. II. Medial, lateral and posterior temporal lobe. *Electroencephalogr Clin Neurophysiol* 1995b;94(4):229–50.
- Hickok G, Poeppel D. Dorsal and ventral streams: a framework for understanding aspects of the functional anatomy of language. *Cognition* 2004;92(1–2):67–99.
- Hillyard SA, Picton TW. *Electrophysiology of cognition*. In: Plum F, editor. *Handbook of physiology*. I. The nervous system. Higher functions of the brain, vol. 5. Bethesda, MD: American Physiological Society; 1987. p. 519–84.
- Hjorth B. An on-line transformation of EEG scalp potentials into orthogonal source derivations. *Electroencephalogr Clin Neurophysiol Suppl* 1975;39(5):526–30.
- Hjorth B. Source derivation simplifies topographical EEG interpretation. *Am J EEG Technol* 1980;20:121–32.
- Holsheimer J. Electrical conductivity of the hippocampal CA1 layers and application to current-source-density analysis. *Exp Brain Res* 1987;67(2):402–10.
- Horn JL. A rationale and test for the number of factors in factor-analysis. *Psychometrika* 1965;30(2):179–85.
- Jasper HH. The ten–twenty electrode system of the international federation. *Electroencephalogr Clin Neurophysiol* 1958;10:371–5.
- Junghöfer M, Elbert T, Leiderer P, Berg P, Rockstroh B. Mapping EEG-potentials on the surface of the brain: a strategy for uncovering cortical sources. *Brain Topogr* 1997;9(3):203–17.

- Junghöfer M, Elbert T, Tucker DM, Braun C. The polar average reference effect: a bias in estimating the head surface integral in EEG recording. *Clin Neurophysiol* 1999;110(6):1149–55.
- Kaiser HF. The application of electronic computers to factor analysis. *Educ Psychol Meas* 1960;20:141–51.
- Kayser J, Tenke CE. Optimizing PCA methodology for ERP component identification and measurement: theoretical rationale and empirical evaluation. *Clin Neurophysiol* 2003;114(12):2307–25.
- Kayser J, Tenke CE. Trusting in or breaking with convention: towards a renaissance of principal components analysis in electrophysiology. *Clin Neurophysiol* 2005;116(8):1747–53.
- Kayser J, Tenke CE. Principal components analysis of Laplacian waveforms as a generic method for identifying ERP generator patterns: II. Adequacy of low-density estimates. *Clin Neurophysiol* 2006;117(2):369–80.
- Kayser J, Tenke C, Nordby H, Hammerborg D, Hugdahl K, Erdmann G. Event-related potential (ERP) asymmetries to emotional stimuli in a visual half-field paradigm. *Psychophysiology* 1997;34(4):414–26.
- Kayser J, Tenke CE, Bruder GE. Dissociation of brain ERP topographies for tonal and phonetic oddball tasks. *Psychophysiology* 1998;35(5):576–90.
- Kayser J, Bruder GE, Friedman D, Tenke CE, Amador XF, Clark SC, Malaspina D, Gorman JM. Brain event-related potentials (ERPs) in schizophrenia during a word recognition memory task. *Int J Psychophysiol* 1999;34(3):249–65.
- Kayser J, Bruder GE, Tenke CE, Stewart JE, Quitkin FM. Event-related potentials (ERPs) to hemifield presentations of emotional stimuli: differences between depressed patients and healthy adults in P3 amplitude and asymmetry. *Int J Psychophysiol* 2000a;36(3):211–36.
- Kayser J, Tenke CE, Bhattacharya N, Stuart BK, Hudson J, Bruder GE. A direct comparison of geodesic sensor net (128-channel) and conventional (30-channel) ERPs in tonal and phonetic oddball tasks. *Psychophysiology* 2000b;37:S17.
- Kayser J, Bruder GE, Tenke CE, Stuart BK, Amador XF, Gorman JM. Event-related brain potentials (ERPs) in schizophrenia for tonal and phonetic oddball tasks. *Biol Psychiatry* 2001;49(10):832–47.
- Kayser J, Fong R, Tenke CE, Bruder GE. Event-related brain potentials during auditory and visual word recognition memory tasks. *Brain Res Cogn Brain Res* 2003a;16(1):11–25.
- Kayser J, Tenke CE, Bruder GE. Evaluating the quality of ERP measures across recording systems: a commentary on Debener et al. (2002). *Int J Psychophysiol* 2003b;48(3):315.
- Keselman HJ. Testing treatment effects in repeated measures designs: an update for psychophysiological researchers. *Psychophysiology* 1998;35(4):470–8.
- Knight RT, Singh J, Woods DL. Pre-movement parietal lobe input to human sensorimotor cortex. *Brain Res* 1989;498:190–4.
- Kok A. Overlap between P300 and movement-related-potentials: a response to Verleger. *Biol Psychol* 1988;27(1):51–8.
- Kutas M, Donchin E. Preparation to respond as manifested by movement-related brain potentials. *Brain Res* 1980;202:95–115.
- Law SK, Rohrbaugh JW, Adams CM, Eckardt MJ. Improving spatial and temporal resolution in evoked EEG responses using surface Laplacians. *Electroencephalogr Clin Neurophysiol* 1993;88(4):309–22.
- Lew GS, Polich J. P300, habituation, and response mode. *Physiol Behav* 1993;53(1):111–7.
- Liegeois-Chauvel C, Musolino A, Badiet JM, Marquis P, Chauvel P. Evoked potentials recorded from the auditory cortex in man: evaluation and topography of the middle latency components. *Electroencephalogr Clin Neurophysiol* 1994;92(3):204–14.
- Logothetis NK, Pauls J, Augath M, Trinath T, Oeltermann A. Neurophysiological investigation of the basis of the fMRI signal. *Nature* 2001;412(6843):150–7.
- Luu P, Tucker DM. Regulating action: alternating activation of midline frontal and motor cortical networks. *Clin Neurophysiol* 2001;112(7):1295–306.
- Luu P, Flaisch T, Tucker DM. Medial frontal cortex in action monitoring. *J Neurosci* 2000;20(1):464–9.
- Luu P, Tucker DM, Derryberry D, Reed M, Poulsen C. Electrophysiological responses to errors and feedback in the process of action regulation. *Psychol Sci* 2003;14(1):47–53.
- Luu P, Tucker DM, Makeig S. Frontal midline theta and the error-related negativity: neurophysiological mechanisms of action regulation. *Clin Neurophysiol* 2004;115(8):1821–35.
- Maiste AC, Wiens AS, Hunt MJ, Scherg M, Picton TW. Event-related potentials and the categorical perception of speech sounds. *Ear Hear* 1995;16(1):68–90.
- Mitzdorf U. Current source-density method and application in cat cerebral cortex: investigation of evoked potentials and EEG phenomena. *Physiol Rev* 1985;65(1):37–100.
- Möcks J, Verleger R. Principal component analysis of event-related potentials: a note on misallocation of variance. *Electroencephalogr Clin Neurophysiol* 1986;65(5):393–8.
- Näätänen R. The role of attention in auditory information processing as revealed by event-related potentials and other brain measures of cognitive function. *Behav Brain Sci* 1990;13:201–88.
- Näätänen R, Picton TW. The N1 wave of the human electric and magnetic response to sound: a review and an analysis of the component structure. *Psychophysiology* 1987;24(4):375–425.
- NeuroScan Inc. STIM software manual. Herndon, VA: Author; 1994.
- Nicholson C. Theoretical analysis of field potentials in anisotropic ensembles of neuronal elements. *IEEE Trans Biomed Eng* 1973;20(4):278–88.
- Nicholson C, Freeman JA. Theory of current source-density analysis and determination of conductivity tensor for anuran cerebellum. *J Neurophysiol* 1975;38(2):356–68.
- Nunez P. *Electric fields of the brain*. New York: Oxford University Press; 1981.
- Nunez PL, Silberstein RB. On the relationship of synaptic activity to macroscopic measurements: does co-registration of EEG with fMRI make sense? *Brain Topogr* 2000;13(2):79–96.
- Nunez PL, Westdorp AF. The surface Laplacian, high resolution EEG and controversies. *Brain Topogr* 1994;6(3):221–6.
- Ohtomo S, Nakasato N, Kanno A, Hatanaka K, Shirane R, Mizoi K, Yoshimoto T. Hemispheric asymmetry of the auditory evoked N100m response in relation to the crossing point between the central sulcus and Sylvian fissure. *Electroencephalogr Clin Neurophysiol* 1998;108(3):219–25.
- Oldfield RC. The assessment and analysis of handedness: the Edinburgh inventory. *Neuropsychologia* 1971;9(1):97–113.
- Oostenveld R, Praamstra P. The five percent electrode system for high-resolution EEG and ERP measurements. *Clin Neurophysiol* 2001;112(4):713–9.
- Pantev C, Bertrand O, Eulitz C, Verkindt C, Hampson S, Schuierer G, Elbert T. Specific tonotopic organizations of different areas of the human auditory cortex revealed by simultaneous magnetic and electric recordings. *Electroencephalogr Clin Neurophysiol* 1995;94(1):26–40.
- Pascual-Marqui RD, Lehmann D. Topographic maps, source localization inference, and the reference electrode: comments on a paper by Desmedt et al. *Electroencephalogr Clin Neurophysiol* 1993;88(6):532–6.
- Perrin F, Pernier J, Bertrand O, Echallier JF. Spherical splines for scalp potential and current density mapping [Corrigenda EEG 02274, *Clin Neurophysiol* 1990;76:565]. *Electroencephalogr Clin Neurophysiol* 1989;72(2):184–7.
- Perrin F, Pernier J, Bertrand O, Echallier JF. Corrigenda EEG 02274. *Electroencephalogr Clin Neurophysiol* 1990;76:565.
- Picton TW, Bentin S, Berg P, Donchin E, Hillyard SA, Johnson Jr R, Miller GA, Ritter W, Ruchkin DS, Rugg MD, Taylor MJ. Guidelines for using human event-related potentials to study cognition: recording standards and publication criteria. *Psychophysiology* 2000;37(2):127–52.

- Polich J. Response mode and P300 from auditory stimuli. *Biol Psychol* 1987;25(1):61–71.
- Roberts LE, Rau H, Lutzenberger W, Birbaumer N. Mapping P300 waves onto inhibition: go/no-go discrimination. *Electroencephalogr Clin Neurophysiol* 1994;92(1):44–55.
- Robinson PA. Neurophysical theory of coherence and correlations of electroencephalographic and electrocorticographic signals. *J Theor Biol* 2003;222(2):163–75.
- Roman R, Brazdil M, Jurak P, Rektor I, Kukleta M. Intracerebral P3-like waveforms and the length of the stimulus-response interval in a visual oddball paradigm. *Clin Neurophysiol* 2005;116(1):160–71.
- Rosburg T, Hauelsen J, Sauer H. Stimulus duration influences the dipole location shift within the auditory evoked field component N100m. *Brain Topogr* 2002;15(1):37–41.
- Salisbury DF, Rutherford B, Shenton ME, McCarley RW. Button-pressing affects P300 amplitude and scalp topography. *Clin Neurophysiol* 2001;112(9):1676–84.
- Salisbury DF, Griggs CB, Shenton ME, McCarley RW. The NoGo P300 ‘anteriorization’ effect and response inhibition. *Clin Neurophysiol* 2004;115(7):1550–8.
- Schroeder CE, Tenke CE, Givre SJ. Subcortical contributions to the surface-recorded flash-VEP in the awake macaque. *Electroencephalogr Clin Neurophysiol* 1992;84:219–31.
- Semlitsch HV, Anderer P, Schuster P, Presslich O. A solution for reliable and valid reduction of ocular artifacts, applied to the P300 ERP. *Psychophysiology* 1986;23(6):695–703.
- Shtyrov Y, Kujala T, Lyytinen H, Ilmoniemi RJ, Näätänen R. Auditory cortex evoked magnetic fields and lateralization of speech processing. *NeuroReport* 2000;11(13):2893–6.
- Sidtis JJ. The complex tone test: implications for the assessment of auditory laterality effects. *Neuropsychologia* 1981;19(1):103–11.
- Simson R, Vaughan HG, Ritter W. The scalp topography of potentials associated with missing visual or auditory stimuli. *Electroencephalogr Clin Neurophysiol* 1976;40(1):33–42.
- Singh J, Knight RT. Frontal lobe contribution to voluntary movements in humans. *Brain Res* 1990;531(1–2):45–54.
- Spencer KM, Dien J, Donchin E. A componential analysis of the ERP elicited by novel events using a dense electrode array. *Psychophysiology* 1999;36(3):409–14.
- Spencer KM, Dien J, Donchin E. Spatiotemporal analysis of the late ERP responses to deviant stimuli. *Psychophysiology* 2001;38(2):343–58.
- Srinivasan R, Nunez PL, Tucker DM, Silberstein RB, Cadusch PJ. Spatial sampling and filtering of EEG with spline Laplacians to estimate cortical potentials. *Brain Topogr* 1996;8(4):355–66.
- Starr A, Aguinaldo T, Roe M, Michalewski HJ. Sequential changes of auditory processing during target detection: motor responding versus mental counting. *Electroencephalogr Clin Neurophysiol* 1997;105(3):201–12.
- Sutton S, Braren M, Zubin J, John ER. Evoked potential correlates of stimulus uncertainty. *Science* 1965;150:1187–8.
- Tandonnet C, Burle B, Hasbroucq T, Vidal F. Spatial enhancement of EEG traces by surface Laplacian estimation: comparison between local and global methods. *Clin Neurophysiol* 2005;116(1):18–24.
- Tenke CE, Kayser J. A convenient method for detecting electrolyte bridges in multichannel electroencephalogram and event-related potential recordings. *Clin Neurophysiol* 2001;112(3):545–50.
- Tenke CE, Kayser J. Reference-free quantification of EEG spectra: Combining current source density (CSD) and frequency principal components analysis (FPCA). *Clin Neurophysiol* 2005;116(12):2826–46.
- Tenke CE, Schroeder CE, Arezzo JC, Vaughan Jr HG. Interpretation of high-resolution current source density profiles: a simulation of sublamina contributions to the visual evoked potential. *Exp Brain Res* 1993;94(2):183–92.
- Tenke CE, Kayser J, Fong R, Leite P, Towey JP, Bruder GE. Response- and stimulus-related ERP asymmetries in a tonal oddball task: a Laplacian analysis. *Brain Topogr* 1998;10(3):201–10.
- The MathWorks Inc. MatLab. The language of technical computing. Version 6.5 (Release 13). Natick, MA: Author; 2002 <http://www.mathworks.com>.
- Tomberg C, Noel P, Ozaki I, Desmedt JE. Inadequacy of the average reference for the topographic mapping of focal enhancements of brain potentials. *Electroencephalogr Clin Neurophysiol* 1990;77(4):259–65.
- van Boxtel GJM. Computational and statistical methods for analyzing event-related potential data. *Behav Res Methods Instrum Comput* 1998;30(1):87–102.
- Vidal F, Hasbroucq T, Grapperon J, Bonnet M. Is the ‘error negativity’ specific to errors? *Biol Psychol* 2000;51(2–3):109–28.
- Vidal F, Grapperon J, Bonnet M, Hasbroucq T. The nature of unilateral motor commands in between-hand choice tasks as revealed by surface Laplacian estimation. *Psychophysiology* 2003;40(5):796–805.
- Wioland N, Rudolf G, Metz-Lutz MN, Mutschler V, Marescaux C. Cerebral correlates of hemispheric lateralization during a pitch discrimination task: an ERP study in dichotic situation. *Clin Neurophysiol* 1999;110(3):516–23.
- Witelson SF, Kigar DL. Asymmetry in brain function follows asymmetry in anatomical form: gross, microscopic, postmortem and imaging studies. In: Boller F, Grafman J, editors. *Handbook of neuropsychology*, vol. 1. Amsterdam: Elsevier; 1988. p. 111–42.
- Wood CC, McCarthy G. Principal component analysis of event-related potentials: simulation studies demonstrate misallocation of variance across components. *Electroencephalogr Clin Neurophysiol* 1984;59(3):249–60.
- Yao D. A method to standardize a reference of scalp EEG recordings to a point at infinity. *Physiol Meas* 2001;22(4):693–711.
- Yao D. High-resolution EEG mapping: a radial-basis function based approach to the scalp Laplacian estimate. *Clin Neurophysiol* 2002a;113(6):956–67.
- Yao D. The theoretical relation of scalp Laplacian and scalp current density of a spherical shell head model. *Phys Med Biol* 2002b;47(12):2179–85.
- Zatorre RJ. Pitch perception of complex tones and human temporal-lobe function. *J Acoust Soc Am* 1988;84(2):566–72.
- Zatorre RJ. Neural specializations for tonal processing. *Ann NY Acad Sci* 2001;930:193–210.
- Zatorre RJ, Evans AC, Meyer E, Gjedde A. Lateralization of phonetic and pitch discrimination in speech processing. *Science* 1992;256:846–9.
- Zhai Y, Yao D. A study on the reference electrode standardization technique for a realistic head model. *Comput Methods Programs Biomed* 2004;76(3):229–38.
- Zouridakis G, Simos PG, Papanicolaou AC. Multiple bilaterally asymmetric cortical sources account for the auditory N1m component. *Brain Topogr* 1998;10(3):183–9.